Multi-Functional RIS for Distributed Over-the-Air Computation in Base Station Free Environments

Ailing Zheng, Wanli Ni, Wen Wang, Hui Tian, Yonina C. Eldar, and Chau Yuen

***Abstract*—Distributed over-the-air computation (AirComp) is a promising technology for fast data aggregation in wireless networks by leveraging multiple access channel to achieve communication and computation simultaneously. However, device-to-device (D2D) links applied are vulnerable to obstacles, and the performance of distributed AirComp is restricted by the device with the worst channel condition. To tackle these issues, we introduce a multi-functional reconfigurable intelligent surface (MF-RIS) to reconstruct the wireless propagation environment, where the MF-RIS can achieve signal reflection, refraction, and amplification simultaneously. Specifically, we propose an MF-RIS-aided distributed AirComp framework, where MF-RIS receives the aggregated data from all devices and then transmits it to each device for post-processing. We formulate a mean-squared error (MSE) minimization problem by jointly optimizing transmit scalar, receive scalar, and MF-RIS coefficients. To address this non-convex problem, we employ an alternating optimization (AO) technique to decompose it into three subproblems, where semi-closed form or closed form solutions are obtained. Then, we extend the single-input single-output (SISO) system into multiple-input multiple-output (MIMO) one. Next, we derive the asymptotic MSE performance for SISO and MIMO cases when the number of RIS elements and that of transmit/receive antennas are very large. Numerical results demonstrate the superiority of MF-RIS in improving MSE performance compared to the baseline without RIS. Additionally, the MF-RIS outperforms its passive counterparts, which reveals the advantages of deploying MF-RIS in distributed AirComp systems to reduce data aggregation error.**

***Index Terms*—Multi-functional reconfigurable intelligent surface, over-the-air computation, mean-square error, transceiver design, alternating optimization.**

I. Introduction

Wireless data aggregation (WDA) is envisioned as a common operation in 5G and beyond communications to support the Internet of Things (IoT), e.g., distributed sensing, learning, and control [1], [2]. To accommodate the growing number of devices under limited radio resources, over-the-air computation (AirComp) has been proposed for WDA [3]. AirComp exploits the co-channel interference among devices to simplify function computation. Specifically, by enabling concurrent data transmission from all devices over the same radio resources and utilizing the signal superposition property of multiple access channels, AirComp directly computes various nomographic functions (e.g., weighted sum, arithmetic mean, geometric mean, and Euclidean norm). Thus, AirComp has been viewed as a potential technique for data aggregation of massive devices in future IoT networks, such as distributed consensus control [4] and federated learning [5]. Traditional AirComp networks consider utilizing a fusion center (FC) to collect the aggregated data and compute the target function under simultaneous data transmission. However, FCs may be absent in certain applications, e.g., autonomous vehicles and cooperative robotics. Thus, distributed AirComp, where each device can recover the target function by messages transmitted from the residual devices without the involvement of FC, has been investigated [6]. Nevertheless, considering that device-to-device (D2D) links are applied in distributed AirComp networks for WDA, which are easily blocked by obstacles, the accuracy of WDA cannot be guaranteed. Furthermore, since the magnitudes of the signals need to be aligned at the receiver, the performance of AirComp systems is limited by the device with the worst channel condition.

Reconfigurable intelligent surface (RIS), an emerging solution to enhance signal propagation conditions by reconfiguring the wireless electromagnetic environment, has attracted attention in recent years [7]. Specifically, by intelligently adjusting the amplitude and phase shift of the incident signals, RIS can effectively redirect them toward the desire direction, thus constructing a smart intelligent electromagnetic environment. Considering that traditional RISs suffer from double-fading attenuation and half-space coverage, which significantly limits the potential of RIS, our previous work proposed a

	SF- RIS		DF- RIS		MF-RIS (This article)
	Reflecting-only RIS	Refracting-only RIS	STAR-RIS	Active RIS	
Signal propagation		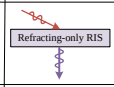	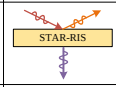	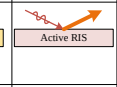	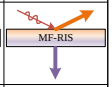
Function support	Reflection	Refraction	Reflection and refraction	Reflection and amplification	Reflection, refraction, and amplification
Full-space coverage	No	No	Yes	No	Yes
Path loss mitigation	No	No	No	Yes	Yes
Thermal noise	No	No	No	Yes	Yes

Fig. 1. MF-RIS versus traditional RISs.

The work of Hui Tian was supported by the Natural Science Foundation of Shandong Province under Grant No. ZR2021LZH010. The work of Chau Yuen was supported by National Research Foundation, Singapore and Infocomm Media Development Authority under its Future Communications Research & Development Programme FCP-NTU-RG-2024-025. The review of this article was coordinated by Prof. Wessam Ajib. (Corresponding author: Hui Tian.)

A. Zheng and H. Tian are with the State Key Laboratory of Networking and Switching Technology, Beijing University of Posts and Telecommunications, Beijing 100876, China (e-mail: {ailing.zheng, tianhui}@bupt.edu.cn).

W. Ni is with Department of Electronic Engineering, Tsinghua University, Beijing 100084, China (e-mail: niwanli@tsinghua.edu.cn).

W. Wang is with the Pervasive Communications Center, Purple Mountain Laboratories, Nanjing 211111, China, and also with the School of Information Science and Engineering, and the National Mobile Communications Research Laboratory, Southeast University, Nanjing 210096, China (email: wangwen@pmlabs.com.cn).

Y. C. Eldar is with the Faculty of Mathematics and Computer Science, Weizmann Institute of Science, Rehovot 7610001, Israel (e-mail: yonina.eldar@weizmann.ac.il).

C. Yuen is with the school of Electrical & Electronic Engineering, Nanyang Technological University, Singapore (e-mail: chau.yuen@ntu.edu.sg).

multi-functional (MF)-RIS, which supports signal reflection, refraction, and amplification simultaneously to mitigate the double-fading attenuation and achieve full-space coverage [8]. Each element of MF-RIS contains an amplifier for signal amplification, a power divider for energy splitting, and two phase shifters for signal redirection, where additional energy is supplied to support the operation of MF-RIS. In Fig. 1, we compare the differences between MF-RIS and traditional RISs, e.g., single-functional (SF)-RIS and dual-functional (DF)-RIS. Therefore, MF-RIS can maintain a desired wireless propagation environment for high-efficient and accurate AirComp, thereby overcoming the bottleneck faced by conventional AirComp systems. Moreover, by constructing virtual links for communications among different devices, MF-RIS can effectively bypass obstacles to provide services for all users, thus reducing computation error. Therefore, introducing MF-RIS into distributed AirComp is a promising technique to improve system performance.

A. Prior Work

1) AirComp-Based Data Aggregation: Due to the capability to fuse communication and computation, AirComp has been investigated extensively to enable efficient data aggregation [3], [9]–[13]. Specifically, the authors of [3] derived a computation-optimal policy of the AirComp system, and investigated the ergodic performance with different Tx-Rx scaling policies. The optimal transceiver design for single-input single-output (SISO) AirComp was investigated in [9], [10]. Then, the authors of [11] proposed a uniform-forcing transceiver design for an AirComp network to compensate the non-uniform channel fading of different devices. Furthermore, to support multi-functional computation, the transmitter design in an multiple-input multiple-output (MIMO) AirComp network was studied in [12], where zero-forcing beamforming and uniform-forcing power control were applied. Then, in [13], the authors designed a MIMO-AirComp equalization and channel feedback technique for spatially multiplexing multifunction computation, thus enabling high-mobility multimodal sensing. In addition, the authors of [14] proposed a hybrid beamforming algorithm, which only relied on the statistical CSI, and provided an asymptotic analysis of mean-squared error (MSE).

Considering the challenges faced by traditional AirComp in addressing the absence of FC, existing works [6] and [15] explored a distributed AirComp framework. Particularly, the authors of [6] proposed the framework of distributed AirComp to achieve a one-step distributed data aggregation in all devices. Moreover, a distributed AirComp based integrated sensing-computation-communication (ISCC) system for multitask collaborative inference was proposed in [15], where the effect of self-interference channel was considered. In addition, since time synchronization is essential for distribute coherent transmission for AirComp to ensure computation accuracy, the AirShare synchronization scheme was proposed in [16] to avoid incoherent transmission.

2) MF-RIS-Aided Wireless Communication: With its ability to reconstruct wireless environments, RISs have been exploited in diverse applications, such as RIS-aided non-orthogonal multiple access (NOMA) [17], [18], physical layer security [19], [20], and integrated sensing and communication (ISAC) [21]. Unfortunately, existing RISs suffer from half-space coverage and double-fading attenuation issues, thus resulting in performance degradation. To overcome the above limitations, our previous works proposed an MF-RIS that supports reflection, refraction, and amplification simultaneously. By embedding reflective and refractive circuits, as well as negative resistance-based amplifiers, MF-RIS achieves full-dimensional communications with enhanced signal power [8]. Existing works [22]–[26] have demonstrated the significant advantages of this novel RIS type over traditional RISs. Specifically, the uplink and downlink MF-RIS-aided communications were investigated in [22], [23] for system throughput maximization, respectively. Three different operating protocols for MF-RIS were proposed in [24]. Moreover, the authors of [25] maximized the communication sum rate under the minimum radar signal-to-noise ratio (SNR) constraint in an MF-RIS-aided ISAC system. In addition, the exact expression of the outage probability for an MF-RIS-aided rate-splitting multiple-access (RSMA) system was derived in [26], where the system throughput and energy efficiency were evaluated in the delay-limited mode.

3) RIS-Aided AirComp Systems: Existing works [27]–[32] introduced RISs into AirComp systems to improve channel conditions and assist data aggregation. Particularly, to address the performance bottleneck caused by the worst channel condition, the authors of [27] introduced RIS to enhance received signals by reconfiguring propagation channels. Then the AirComp distortion was minimized by designing AirComp transceivers and RIS phase-shifts. Moreover, in [28], a two-stage stochastic beamforming algorithm was proposed to reduce the heavy channel state information (CSI) signaling overhead, where the average computation MSE was minimized by updating the long-term passive RIS beamforming matrix based on the channel statistics. Furthermore, the authors of [29] considered an additive bounded CSI uncertainty in a RIS-aided AirComp system, where the worst-case design of transceivers and RIS phase was studied for MSE minimization. Moreover, the RIS-aided AirComp for WDA in mmWave system was investigated in [30], which derived the closed-form expressions of transmit scalars. To achieve a full-space coverage, the authors of [31] studied a simultaneously transmitting and reflecting reconfigurable intelligent surfaces (STAR-RIS)-aided AirComp system, where STAR-RIS coefficients, and the transmit and receive beamforming were optimized jointly. Furthermore, to alleviate the double-fading attenuation, the asymptotic MSE of active RIS-aided AirComp systems was derived in [32], where the self-interference caused by the full-duplex mode was studied. The above literature focus on RIS-aided traditional centralized AirComp systems, where FC is deployed for WDA. Considering that distributed AirComp is an important direction for future applications, e.g., D2D communications and distributed federated edge learning, and data aggregation via D2D links between each device is vulnerable to obstacles, the authors of [33] introduced RISs into distributed AirComp systems, where RIS was applied to achieve communications among different devices for efficient

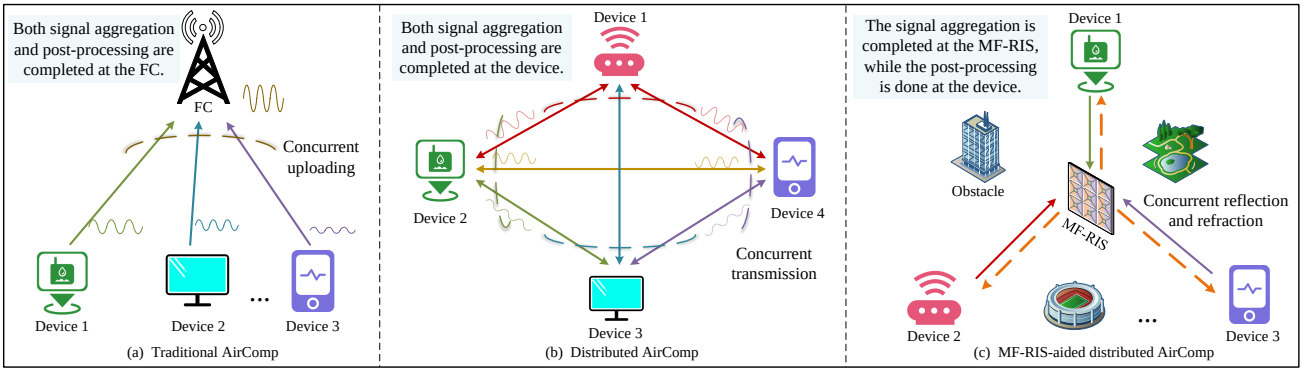

Fig. 2. Traditional AirComp vs. the proposed MF-RIS-aided distributed AirComp systems.

target function computation. Unfortunately, the RIS in [33] only reflects the impinging signals, which suffers from double-fading attenuation issue and can not be applied to scenarios where devices are distributed throughout the range. Inspired by our previous works [34] and [35] which provide the related hardware design, the proposed MF-RIS can extend RIS coverage and enhance signal strength for users located in full space. Thus, we introduce MF-RISs into distributed AirComp systems to overcome these limitations in this paper, which remains unexplored in the current research.

B. Contributions and Organization

Based on the above, by reflecting, refracting, and amplifying the incident signals simultaneously, MF-RIS is able to assist distributed AirComp systems to overcome the bottleneck caused by the device with the worst channel condition, and construct virtual links for communications among different devices. Thus, we investigate an MF-RIS-aided distributed AirComp system in this paper. The aim is to minimize the average computation MSE between the target and estimated function values. Our main contributions are summarized as follows:

- We propose an MF-RIS-aided distributed AirComp system, where devices are distributed around the MF-RIS. Then, we formulate an MSE minimization problem by jointly designing the transmit and receive scalar, and MF-RIS coefficients. Due to the non-convex objective function and coupled variables, the formulated problem is challenging to solve directly. Thus, we apply an alternating optimization (AO) framework to decompose the original problem into three subproblems, such that each subproblem can be solved efficiently.
- For generality, we extend the SISO system into MIMO one, where all devices are equipped with multiple antennas. Based on the MIMO setup, multiple arithmetic mean functions of the recorded signals from all devices can be computed. Then, we minimize the MSE problem by jointly optimizing the transmit and receive beamforming, and MF-RIS coefficients. For both SISO and MIMO cases, we derive the asymptotic expressions of MSE when the number of RIS elements is sufficiently large.
- Numerical results verify the superiority of MF-RIS-aided distributed AirComp system. The MF-RIS achieves the lowest MSE performance when varying the number of RIS elements, devices, and antennas. Besides, the MIMO case with more spatial diversity outperforms the SISO one, with a 28% reduction in MSE. In addition, compared to distributed AirComp scheme without RIS, the RIS-aided schemes obtain a 40% MSE decrease.

The remainder of this paper is organized as follows. In Section II, we introduce the system model of MF-RIS-aided distributed AirComp and formulate an MSE minimization problem. Section III presents the AO algorithm to address the formulated problem. Then, Section IV extends the SISO case into the MIMO one for general configuration. Subsequently, in Section V, we analyze the asymptotic performance of the considered MF-RIS-aided distributed AirComp system. Numerical results are provided in Section VI. Finally, Section VII draws the conclusion.

Notations: Throughout the paper, we adopt the boldface lowercase letters for vectors and boldface uppercase letters for matrices, respectively. $\mathbf{X}^*$, $\mathbf{X}^{\mathrm{T}}$, $\mathbf{X}^{\mathrm{H}}$, and $\|\mathbf{X}\|_F$ denote the conjugate, transpose, Hermitian, Frobenius norm of matrix $\mathbf{X}$, respectively. $\|\mathbf{x}\|$ denotes 2-norm of vector $\mathbf{x}$. $\mathrm{diag}(\mathbf{x})$ denotes a diagonal matrix with the entries of $\mathbf{X}$ on its main diagonal; $\mathrm{diag}(\mathbf{X})$ is the main diagonal of $\mathbf{X}$. In addition, $[\mathbf{x}]_n$ denotes the n-th element of vector $\mathbf{x}$ and $[\mathbf{X}]_{n:n+l}$ denotes the column data from row n to row l. $\mathbf{I}$ denotes the identity matrix. $\mathbb{E}$ is the expectation operator. $\mathrm{Re}\{\cdot\}$ and $\mathrm{Tr}\{\cdot\}$ denote the real part and trace of a complex number, respectively. $\odot$ represent the Hadamard product.

II. System Model

We consider an MF-RIS-assisted distributed AirComp system, as shown in Fig. 2, which consists of N devices and an MF-RIS equipped with M elements. Specifically, the devices are divided into two groups, i.e., R and T groups, where the devices in R (T) group are located in reflection (refraction) space. The sets of elements and devices are denoted by $\mathcal{M} = \{1, 2, \ldots, M\}$ and $\mathcal{N} = \{1, 2, \ldots, N\}$, respectively, where the sets of devices in reflection and refraction spaces are denoted by $\mathcal{N}_r$ and $\mathcal{N}_t$ with $N_r + N_t = N$. Besides, we have the set of space as $\mathcal{C} = \{r, t\}$. In this distributed AirComp system, each device is responsible for transmitting its own data and receiving an aggregation of all the data. Moreover, by exploiting AirComp technique, we assume that

the synchronization of different devices is established [16]. For simplicity, we assume that direct links between devices are blocked to provide a more concise system model, which helps to gain performance insights in subsequent sections. Thus, each device can only communicate with each other via MF-RIS. In addition, the existing system model can be easily extended to systems with D2D links. Let $s_i \in \mathbb{C}$ denote the transmit signal of device i. The signal s_i is assumed to be normalized and independent among devices, i.e., $\mathbb{E}(s_i s_i^*) = 1$ and $\mathbb{E}(s_i s_j^*) = 0, \forall i \neq j \in \mathcal{N}$. The receiver is expected to compute the average value of the data sent by all devices. We have

$$s = \frac{1}{N} \sum\nolimits_{i \in \mathcal{N}} s_i. \tag{1}$$

Notice that the MF-RIS only redirects incident signals from each device, and the post-processing of the aggregated information is completed at the device side. Considering that each device transmits and receives data simultaneously, we assume that each device is equipped with one transmit antenna and one receive antenna, and all devices operate in full-duplex mode. Moreover, transmit and receive antennas within the same device are considered to be perfectly decoupled through self-interference (SI) cancellation techniques [36]. Furthermore, we assume that the SI at the MF-RIS can be perfectly suppressed [37]. Denote v_i as the transmit coefficient at device i, then the corresponding transmitted signal is given by

$$x_i = v_i s_i. \tag{2}$$

The signal relayed by the MF-RIS can be expressed as

$$\mathbf{x}_{\mathrm{RIS}} = \mathbf{\Theta}_r \left(\sum\nolimits_{i \in \mathcal{N}_r} \mathbf{h}_i x_i + \mathbf{z} \right) + \mathbf{\Theta}_t \left(\sum\nolimits_{i \in \mathcal{N}_t} \mathbf{h}_i x_i + \mathbf{z} \right), \tag{3}$$

where $\mathbf{h}_i \in \mathbb{C}^{M \times 1}$ is the reciprocal channel between device i and MF-RIS. We assume that the perfect CSI can be obtained to provide an upper bound of the system performance[1]. Specifically, the CSI estimation is handled by a device with strong computing capabilities, referred to as the leader device (LD), which is also responsible for solving the optimization problem[2]. $\mathbf{\Theta}_c = \mathrm{diag}(\mathbf{u}_c)$ represents the MF-RIS coefficients for the reflection ($c = r$) and refraction ($c = t$) spaces, with $\mathbf{u}_c = [\sqrt{\beta_1^c} e^{j\theta_1^c}, \sqrt{\beta_2^c} e^{j\theta_2^c}, \ldots, \sqrt{\beta_M^c} e^{j\theta_M^c}]^{\mathrm{T}}$ and $c \in \mathcal{C}$. Moreover, $\beta_m^{r/t} \in [0, \beta_{\max}]$ and $\theta_m^{r/t} \in [0, 2\pi]$ represent the amplitude and phase of the m-th MF-RIS element, where $\beta_{\max} \geq 1$ denotes the maximum amplification factor. Due to the law of energy conservation, we have $\beta_m^r + \beta_m^t \leq \beta_{\max}$. Here $\mathbf{z} \in \mathbb{C}^{M \times 1} \sim \mathcal{CN}(0, \sigma_s^2 \mathbf{I}_M)$ denotes the thermal noise at the MF-RIS with each element's noise power σ_s^2. Assuming the maximum transmit power of device i is P_i, we have

$$\mathbb{E}[|v_i s_i|^2] = |v_i|^2 \leq P_i, \quad \forall i \in \mathcal{N}. \tag{4}$$

[1]Note that the perfect CSI is difficult to obtain in practical scenarios, and the optimization under imperfect CSI is similar to [29], [38].

[2]When the base station (BS) is involved, it collects all estimated CSI during the initial stage, solves the optimization problem, and then distributes the optimization results to all devices and the MF-RIS.

Thus, the signal received at device i in space c is given by

$$\begin{aligned} \hat{s}_{c,i} =& a_i \Big(\mathbf{h}_i^{\mathrm{H}} \mathbf{\Theta}_c \mathbf{h}_i x_i + \sum\nolimits_{n \in \mathcal{N}_c \setminus \{i\}} \mathbf{h}_i^{\mathrm{H}} \mathbf{\Theta}_c \mathbf{h}_n x_n \\ &+ \sum\nolimits_{n \in \mathcal{N}_{\bar{c}}} \mathbf{h}_i^{\mathrm{H}} \mathbf{\Theta}_{\bar{c}} \mathbf{h}_n x_n + \sum\nolimits_{j \in \mathcal{C}} \mathbf{h}_i^{\mathrm{H}} \mathbf{\Theta}_j \mathbf{z} + z_i \Big), \end{aligned} \tag{5}$$

where a_i is the reception scaling factors of device i, and $z_i \sim \mathcal{CN}(0, \sigma_i^2)$ represents the thermal noise at device i. If $c = r$, we have $\bar{c} = t$, and otherwise. Then the computational distortion at device i, which is measured by the MSE between $\hat{s}_{c,i}$ and s, is given by

$$\begin{aligned} \mathrm{MSE}_i =& \mathbb{E}[|\hat{s}_{c,i} - s|^2] \\ =& \sum\nolimits_{c \in \mathcal{C}} \Big(\sum\nolimits_{n \in \mathcal{N}_c} \Big| \Big(a_i \mathbf{h}_i^{\mathrm{H}} \mathbf{\Theta}_c \mathbf{h}_n v_n - \frac{1}{N} \Big) \Big|^2 \\ &+ \sigma_s^2 \| a_i \mathbf{h}_i^{\mathrm{H}} \mathbf{\Theta}_c \|^2 \Big) + |a_i|^2 \sigma_i^2. \end{aligned} \tag{6}$$

In this work, we aim to minimize the average MSE of all users. Therefore, the optimization problem is formulated as

$$\min_{\mathbf{a}, \mathbf{v}, \mathbf{\Theta}_c} \frac{1}{N} \sum\nolimits_{i \in \mathcal{N}} \mathrm{MSE}_i(v_i, a_i, \mathbf{\Theta}_c) \tag{7a}$$

$$\text{s.t.} \quad |v_i|^2 \leq P_i, \tag{7b}$$

$$\|\mathbf{x}_{\mathrm{RIS}}\|^2 \leq P_{\mathrm{RIS}}, \tag{7c}$$

$$\beta_m^{r/t} \in [0, \beta_{\max}], \beta_m^r + \beta_m^t \leq \beta_{\max}, \theta_m^{r/t} \in [0, 2\pi], \tag{7d}$$

where $\mathbf{a} = [a_1, a_2, \cdots, a_N]^{\mathrm{T}}$ and $\mathbf{v} = [v_1, v_2, \cdots, v_N]^{\mathrm{T}}$. Here P_{RIS} denotes the amplification power budget at the MF-RIS[3]. Specifically, constraint (7d) defines the range of values for MF-RIS coefficients and indicates that MF-RIS supports signal amplification, reflection, and refraction simultaneously. Owing to the non-convex objective function (7a) and coupled variables, problem (7) is difficult to solve directly. Therefore, we apply an alternating optimization (AO) framework to address it in the following.

III. Algorithm Design for SISO-AirComp System

A. Optimization of Transmit Scalar

In this subsection, we optimize the transmit scalar $\mathbf{v}$ with fixed $\{\mathbf{a}, \mathbf{\Theta}_c\}$. The corresponding optimization subproblem is

$$\min_{\mathbf{v}} \ \frac{1}{N} \sum\nolimits_{i \in \mathcal{N}} \mathrm{f}_i(\mathbf{v}) \tag{8a}$$

$$\text{s.t.} \ \ (7\text{b}), \ (7\text{c}), \tag{8b}$$

where $\mathrm{f}_i(\mathbf{v}) = \sum_{c \in \mathcal{C}} \sum_{n \in \mathcal{N}_c} |(a_i \mathbf{h}_i^{\mathrm{H}} \mathbf{\Theta}_c \mathbf{h}_n v_n - \frac{1}{N})|^2$.

Let $\mathbf{v}_c = [v_1, v_2, \cdots, v_{N_c}]$, $\mathbf{V}_c = \mathrm{diag}(\mathbf{v}_c)$, and $\widehat{\mathbf{H}}_{c,i} = [H_{1,i,c}, H_{2,i,c}, \cdots, H_{N_c,i,c}]$, where $H_{n,i,c} = \mathbf{h}_i^{\mathrm{H}} \mathbf{\Theta}_c \mathbf{h}_n$ denotes the equivalent channel from device n to device i. Then we get

$$\mathrm{f}_i(\mathbf{v}) = \sum\nolimits_{c \in \mathcal{C}} \left\| a_i \mathbf{V}_c^{\mathrm{H}} \widehat{\mathbf{H}}_{c,i}^{\mathrm{H}} - \frac{1}{N} \mathbf{I}_{N_c \times 1} \right\|^2. \tag{9}$$

[3]The average MSE minimization problem can be transformed into a min-max problem by directly converting the objective function. Due to their similarity, the proposed algorithm can be extended to solve the min-max problem easily.

Then, the objective function of problem (8) is modified as

$$\frac{1}{N}\sum_{i\in\mathcal{N}}\mathrm{f}_i(\mathbf{v}) = \frac{1}{N}\sum_{c\in\mathcal{C}}\sum_{i\in\mathcal{N}}\Big(a_i^2\mathrm{Tr}\Big(\mathbf{V}_c^{\mathrm{H}}\widehat{\mathbf{H}}_{c,i}^{\mathrm{H}}\widehat{\mathbf{H}}_{c,i}\mathbf{V}_c\Big) - 2\,\mathrm{Re}\Big\{\frac{1}{N}a_i\mathrm{Tr}\Big(\mathbf{I}_{N_c\times 1}\widehat{\mathbf{H}}_{c,i}\mathbf{V}_c\Big)\Big\} + (\frac{1}{N})^2\Big).$$

For constraint (7c), we have

$$\sum\nolimits_{c\in\mathcal{C}}\Big(\mathrm{Tr}\Big(\mathbf{V}_c^{\mathrm{H}}\mathbf{H}_c^{\mathrm{H}}\mathbf{\Theta}_c^{\mathrm{H}}\mathbf{\Theta}_c\mathbf{H}_c\mathbf{V}_c\Big) + \sigma_s^2\|\mathbf{\Theta}_c\|_F^2\Big) \le P_{\mathrm{RIS}}, \quad (10)$$

where $\mathbf{H}_c = [\mathbf{h}_1, \mathbf{h}_2, \cdots, \mathbf{h}_{N_c}]$. Since $\mathbf{V}_c$ is a diagonal matrix, problem (8) is reformulated as

$$\min_{\mathbf{v}} \ \mathbf{v}^{\mathrm{H}}\widetilde{\mathbf{H}}\mathbf{v} - 2\,\mathrm{Re}\{\mathbf{B}\mathbf{v}\} \quad (11a)$$

$$\text{s.t.} \ \ \mathbf{v}^{\mathrm{H}}\mathbf{C}\mathbf{v} \le P_{\mathrm{RIS}} - \sum\nolimits_{c\in\mathcal{C}}\sigma_s^2\|\mathbf{\Theta}_c\|_F^2, \ (7b), \quad (11b)$$

where $\bar{\mathbf{H}}_c = \sum_{i\in\mathcal{N}} a_i\mathbf{I}_{N_c\times 1}\widehat{\mathbf{H}}_{c,i}$, with

$$\widetilde{\mathbf{H}} = \begin{bmatrix} \frac{1}{N}\sum\limits_{i\in\mathcal{N}} a_i^2\Big(\widehat{\mathbf{H}}_{r,i}^{\mathrm{H}}\widehat{\mathbf{H}}_{r,i}\Big)\odot\mathbf{I} & \mathbf{0} \\ \mathbf{0} & \frac{1}{N}\sum\limits_{i\in\mathcal{N}} a_i^2\Big(\widehat{\mathbf{H}}_{t,i}^{\mathrm{H}}\widehat{\mathbf{H}}_{t,i}\Big)\odot\mathbf{I} \end{bmatrix},$$

$$\mathbf{C} = \begin{bmatrix} \mathbf{H}_r^{\mathrm{H}}\mathbf{\Theta}_r^{\mathrm{H}}\mathbf{\Theta}_r\mathbf{H}_r\odot\mathbf{I} & \mathbf{0} \\ \mathbf{0} & \mathbf{H}_t^{\mathrm{H}}\mathbf{\Theta}_t^{\mathrm{H}}\mathbf{\Theta}_t\mathbf{H}_t\odot\mathbf{I} \end{bmatrix}, \mathbf{v} = \begin{bmatrix}\mathbf{v}_r & \mathbf{v}_t\end{bmatrix}^{\mathrm{H}},$$

$$\mathbf{B} = \frac{1}{N^2}[[\bar{\mathbf{H}}_r]_{1,1}, \cdots, [\bar{\mathbf{H}}_r]_{N_r,N_r}, [\bar{\mathbf{H}}_t]_{1,1}, \cdots, [\bar{\mathbf{H}}_t]_{N_t,N_t}].$$

If constraint (7b) is ignored, the closed form solution of problem (11) is given by

$$\mathbf{v}^\star = (\widetilde{\mathbf{H}} + \lambda\mathbf{C})^{-1}\mathbf{B}^{\mathrm{H}}, \quad (12)$$

where $\lambda \ge 0$ is the introduced Lagrange dual variable for the first term in constraint (11b). Considering constraint (7b), the solution of $\mathbf{v}$ is modified as

$$v_n^o = \frac{[\mathbf{v}]_n^\star}{|[\mathbf{v}]_n^\star|}\min(\sqrt{P_n}, |[\mathbf{v}]_n^\star|), \ \forall n \in \mathcal{N}. \quad (13)$$

The solution of ${v_n}^o$ in (13) is the optimal solution to problem (11) [39]. The detailed analysis is given in Appendix A. The optimal λ can be found by the bisection search to ensure the first term in constraint (11b). The lower bound of λ is $\lambda_{LB} = 0$, while the upper bound of λ is obtained as

$$\lambda \le \lambda_{UB} = \sqrt{\frac{\mathbf{B}\mathbf{C}^{-1}\mathbf{B}^{\mathrm{H}}}{P_{\mathrm{RIS}} - \sigma_s^2\sum_{c\in\mathcal{C}}\|\mathbf{\Theta}_c\|^2}}. \quad (14)$$

B. Optimization of MF-RIS Coefficients

With fixed $\{\mathbf{a}, \mathbf{v}\}$, the corresponding optimization subproblem with respect to $\mathbf{\Theta}_c$ is given by

$$\min_{\mathbf{\Theta}_c} \ \frac{1}{N}\sum\nolimits_{i\in\mathcal{N}}\mathrm{MSE}_i(\mathbf{\Theta}_c) \quad (15a)$$

$$\text{s.t.} \ \ (7c), (7d). \quad (15b)$$

By utilizing $\mathbf{\Theta}_c\mathbf{x} = \mathrm{diag}(\mathbf{x})\mathbf{u}_c$, problem (15) is equivalently transformed into

$$\min_{\mathbf{u}_c} \frac{1}{N}\sum_{c\in\mathcal{C}}\Big(\mathbf{u}_c^{\mathrm{H}}\sum_{i\in\mathcal{N}}\mathbf{Q}_{c,i}\mathbf{u}_c - \frac{2}{N}\,\mathrm{Re}\Big\{\sum_{i\in\mathcal{N}}\mathbf{r}_{c,i}^{\mathrm{H}}\mathbf{u}_c\Big\}\Big) \quad (16a)$$

$$\text{s.t.} \ \sum\nolimits_{c\in\mathcal{C}}\mathbf{u}_c^{\mathrm{H}}\mathbf{U}_c\mathbf{u}_c \le P_{\mathrm{RIS}}, (7d), \quad (16b)$$

where $\mathbf{Q}_{c,i}$, $\mathbf{r}_{c,i}$, and $\mathbf{U}_c$ are given by

$$\mathbf{Q}_{c,i} = \mathbf{r}_{c,i}\mathbf{r}_{c,i}^{\mathrm{H}} + \sigma_s^2\mathrm{diag}(a_i\mathbf{h}_i^{\mathrm{H}})\mathrm{diag}(\mathbf{h}_i a_i),$$
$$\mathbf{U}_c = \sum\nolimits_{n\in\mathcal{N}_c}|v_n|^2\mathrm{diag}(\mathbf{h}_n^{\mathrm{H}})\mathrm{diag}(\mathbf{h}_n) + \sigma_s^2\mathbf{I}_{M\times M},$$
$$\mathbf{r}_{c,i} = \sum\nolimits_{n\in\mathcal{N}_c} a_i\mathrm{diag}(\mathbf{h}_n^{\mathrm{H}}v_n)\mathbf{h}_i.$$

By omitting constraint (7d), the Lagrange dual function of problem (16) is given by

$$\mathcal{L} = \mathbf{u}^{\mathrm{H}}\mathbf{Q}\mathbf{u} - \frac{2}{N}\,\mathrm{Re}\{\mathbf{r}^{\mathrm{H}}\mathbf{u}\} + \zeta(\mathbf{u}^{\mathrm{H}}\mathbf{U}\mathbf{u} - P_{\mathrm{RIS}}), \quad (17)$$

where $\zeta \ge 0$ is the introduced Lagrange dual variable for the first term in constraint (16b). Here we have

$$\mathbf{u} = [\mathbf{u}_r; \mathbf{u}_t], \mathbf{r} = \Big[\sum\nolimits_{i\in\mathcal{N}}\mathbf{r}_{r,i}^{\mathrm{H}}, \sum\nolimits_{i\in\mathcal{N}}\mathbf{r}_{t,i}^{\mathrm{H}}\Big]^{\mathrm{H}},$$
$$\mathbf{U} = \begin{bmatrix}\mathbf{U}_r & \mathbf{0}\\ \mathbf{0} & \mathbf{U}_t\end{bmatrix}, \mathbf{Q} = \begin{bmatrix}\sum_{i\in\mathcal{N}}\mathbf{Q}_{r,i} & \mathbf{0}\\ \mathbf{0} & \sum_{i\in\mathcal{N}}\mathbf{Q}_{t,i}\end{bmatrix}.$$

Then by calculating the first-order partial derivation of $\mathcal{L}$ regarding to $\mathbf{u}$, we obtain

$$\frac{\partial\mathcal{L}}{\partial\mathbf{u}} = 2(\mathbf{Q} + \zeta\mathbf{U})\mathbf{u} - \frac{2}{N}\mathbf{r}. \quad (18)$$

Thus, we have the closed form solution to problem (16) as

$$\mathbf{u}^\star = \frac{1}{N}(\mathbf{Q} + \zeta\mathbf{U})^{-1}\mathbf{r}. \quad (19)$$

To obtain ζ, when the first term in constraint (16b) is inactive, we set $\zeta = 0$. If the first term in constraint (16b) is active, we have $\mathbf{u}^{\mathrm{H}}\mathbf{U}\mathbf{u} = P_{\mathrm{RIS}}$. Then the optimal ζ can be found by the bisection search to ensure $\mathbf{u}^{\mathrm{H}}\mathbf{U}\mathbf{u} = P_{\mathrm{RIS}}$. The lower bound on ζ is $\zeta_{LB} = 0$. For the upper bound of ζ, we have

$$\Big(\frac{1}{N}(\mathbf{Q} + \zeta\mathbf{U})^{-1}\mathbf{r}\Big)^{\mathrm{H}}\mathbf{U}\Big(\frac{1}{N}(\mathbf{Q} + \zeta\mathbf{U})^{-1}\mathbf{r}\Big) = P_{\mathrm{RIS}}. \quad (20)$$

Since $\zeta\mathbf{U} \preceq \mathbf{Q} + \zeta\mathbf{U}$, we get

$$(\frac{1}{N})^2(\zeta^{-1}\mathbf{U}^{-1}\mathbf{r})^{\mathrm{H}}\mathbf{U}(\zeta^{-1}\mathbf{U}^{-1}\mathbf{r}) \ge P_{\mathrm{RIS}}. \quad (21)$$

Since $\mathbf{U}$ is a Hermitian matrix, we obtain

$$\zeta \le \zeta_{UB} = \sqrt{\frac{\mathbf{r}^{\mathrm{H}}\mathbf{U}^{-1}\mathbf{r}}{N^2P_{\mathrm{RIS}}}}. \quad (22)$$

Considering constraint (7d), we have the modified solution of $\mathbf{u}$ as follows

$$\mathbf{u}_{c,m}^o = \frac{[\mathbf{u}^\star]_{c,m}}{|[\mathbf{u}^\star]_{c,m}|}\min\left(\sqrt{\frac{\mathbf{u}_{c,m}^{\star,2}}{\mathbf{u}_{c,m}^{\star,2} + \mathbf{u}_{\bar{c},m}^{\star,2}}}\beta_{\max}, |[\mathbf{u}^\star]_{c,m}|\right). \quad (23)$$

The solution of $\mathbf{u}_{c,m}^o$ in (23) is the optimal solution to problem (16), which is similar to the analysis of $\mathbf{v}$.

C. Optimization of Receive Scalar

In this subsection, we optimize receive scalar $\mathbf{a}$ with fixed $\{\mathbf{v}, \mathbf{\Theta}_c\}$. The corresponding optimization problem is given by

$$\min_{\mathbf{a}} \ \frac{1}{N}\sum\nolimits_{i\in\mathcal{N}}\mathrm{MSE}_i(a_i) \quad (24)$$

Algorithm 1 The AO Algorithm for Solving Problem (7)

1: **Initialize** $\mathbf{v}^{(0)}$, $\mathbf{\Theta}^{(0)}$, $\mathbf{a}^{(0)}$, the maximum number of iteration $T_{\max}$, and the predefined threshold ϵ.
2: **repeat**
3: Set the iteration index $\tau = 0$;
4: Given $\mathbf{a}^{(\tau)}$ and $\mathbf{\Theta}^{(\tau)}$, update $\mathbf{v}^{(\tau+1)}$ via (13);
5: Given $\mathbf{a}^{(\tau)}$ and $\mathbf{v}^{(\tau+1)}$, update $\mathbf{\Theta}^{(\tau+1)}$ via (19);
6: Given $\mathbf{v}^{(\tau+1)}$ and $\mathbf{\Theta}^{(\tau+1)}$, update $\mathbf{a}^{(\tau+1)}$ via (25);
7: Update $\tau = \tau + 1$;
8: **until** $|\mathrm{MSE}^{(\tau)} - \mathrm{MSE}^{(\tau-1)}| \leq \epsilon$ or $\tau \geq T_{\max}$;
9: **Output** the converged solutions $\mathbf{v}$, $\mathbf{\Theta}$, and $\mathbf{a}$.

Taking the first-order partial derivative of $\mathrm{MSE}_i(a_i)$ regarding to a_i, we have

$$\begin{aligned}\frac{\partial \mathrm{MSE}_i(a_i)}{\partial a_i} =& 2a_i\Big(\sum\nolimits_{n\in\mathcal{N}_r}|v_n H_{n,i,r}|^2+\sigma_s^2(\mathbf{h}_i^{\mathrm{H}}\mathbf{\Theta}_r\mathbf{\Theta}_r^{\mathrm{H}}\mathbf{h}_i)\\ &+\sum\nolimits_{n\in\mathcal{N}_t}|v_n H_{n,i,t}|^2+\sigma_s^2(\mathbf{h}_i^{\mathrm{H}}\mathbf{\Theta}_t\mathbf{\Theta}_t^{\mathrm{H}}\mathbf{h}_i)+\sigma_i^2\Big)\\ &-\frac{2}{N}\Big(\sum\nolimits_{n\in\mathcal{N}_r}H_{n,i,t}v_n+\sum\nolimits_{n\in\mathcal{N}_t}H_{n,i,t}v_n\Big),\ \forall i.\end{aligned}$$

Then the closed form solution of the optimal a_i can be obtained by solving $\frac{\partial \mathrm{MSE}(a_i)}{\partial a_i} = 0$. Thus, we have

$$\begin{aligned}a_i =& \Big(\sum\nolimits_{c\in\mathcal{C}}\Big(\sum\nolimits_{n\in\mathcal{N}_c}|v_n H_{n,i,c}|^2+\sigma_s^2(\mathbf{h}_i^{\mathrm{H}}\mathbf{\Theta}_c\mathbf{\Theta}_c^{\mathrm{H}}\mathbf{h}_i)\Big)+\sigma_i^2\Big)^{-1}\\ &\times\frac{1}{N}\Big(\sum\nolimits_{c\in\mathcal{C}}\sum\nolimits_{n\in\mathcal{N}_c}H_{n,i,c}v_n\Big),\ \forall i. \end{aligned}\tag{25}$$

The overall alternating optimization algorithm is summarized in Algorithm 1.

D. Analysis of Complexity and Convergence

For the calculation of $\mathbf{a}, \mathbf{v}$, and $\mathbf{\Theta}$, the complexities are $\mathcal{O}(1)$, $\mathcal{O}(N^3)$, and $\mathcal{O}(8M^3)$, respectively, which are mainly on the matrix inversions. The optimizations of $\mathbf{v}$ and $\mathbf{\Theta}$ employ the bisection search, thus the computational complexities are

$$\mathcal{O}(N^3)\log_2\left(\frac{\lambda_{UB}}{\epsilon}\right) \text{ and } \mathcal{O}(8M^3)\log_2\left(\frac{\zeta_{UB}}{\epsilon}\right),\tag{26}$$

where ϵ is the bisection search accuracy. Therefore, the computational complexity of the proposed AO algorithm is

$$\mathcal{O}\Big(T\Big(N^3\log_2\left(\frac{\lambda_{UB}}{\epsilon}\right)+8M^3\log_2\left(\frac{\zeta_{UB}}{\epsilon}\right)\Big)\Big),\tag{27}$$

where T denotes the iteration number for convergence.

Theorem 1. *Algorithm 1 converges to a locally optimal point of problem (7) over several iterations.*

Proof. To prove the convergence of Algorithm 1, we have

$$\begin{aligned}\mathrm{MSE}\Big(\mathbf{v}^{(\tau)},\mathbf{\Theta}^{(\tau)},\mathbf{a}^{(\tau)}\Big) &\overset{(a)}{\geq} \mathrm{MSE}\Big(\mathbf{v}^{(\tau+1)},\mathbf{\Theta}^{(\tau)},\mathbf{a}^{(\tau)}\Big)\\ &\overset{(b)}{\geq} \mathrm{MSE}\Big(\mathbf{v}^{(\tau+1)},\mathbf{\Theta}^{(\tau+1)},\mathbf{a}^{(\tau)}\Big)\\ &\overset{(c)}{\geq} \mathrm{MSE}\Big(\mathbf{v}^{(\tau+1)},\mathbf{\Theta}^{(\tau+1)},\mathbf{a}^{(\tau+1)}\Big),\end{aligned}\tag{28}$$

where τ denotes the iteration index. Here, (a), (b), and (c) follow since the updates of $\mathbf{v}$, $\mathbf{\Theta}$, and $\mathbf{a}$ minimize MSE when the other variables are fixed. Moreover, considering that $\mathrm{MSE}(\mathbf{v},\mathbf{\Theta},\mathbf{a})$ is monotonically non-increasing in each iteration and its value is lower bounded by zero, Algorithm 1 will converge to a local optimum of problem (7) after several iterations. □

IV. Extension to MIMO-AirComp System

In this section, to investigate the MSE performance when multiple messages need to be transmitted, where multiple antennas are deployed at each device, we extend the SISO case into the MIMO one. For simplicity, we assume that each device is equipped with the same number of transmit and receive antennas, i.e., N_s.

A. System Model

In MIMO AirComp system, each device transmits L parameters with $L \leq N_s$ and $L \geq 1$. Denote the signal of the i-th device as $\mathbf{s}_i \in \mathbb{C}^{L\times 1}$, satisfying $\mathbb{E}(\mathbf{s}_i\mathbf{s}_i^{\mathrm{H}}) = \mathbf{I}_L$ and $\mathbb{E}(\mathbf{s}_i\mathbf{s}_j^{\mathrm{H}}) = \mathbf{0}$, $\forall i \neq j \in \mathcal{N}$. We take calculating the average value of all data as the target function, i.e.,

$$\mathbf{s} = \frac{1}{N}\sum\nolimits_{i\in\mathcal{N}}\mathbf{s}_i.\tag{29}$$

Let $\mathbf{W}_i \in \mathbb{C}^{N_s\times L}$ and $\mathbf{G}_i \in \mathbb{C}^{M\times N_s}$ denote the transmit beamforming matrix at the i-th device and the channel from the i-th device to the MF-RIS. The signal received at the MF-RIS is given by

$$\mathbf{x}_{\mathrm{RIS}} = \sum\nolimits_{c\in\mathcal{C}}\Big(\mathbf{\Theta}_c\Big(\sum\nolimits_{i\in\mathcal{N}_c}\mathbf{G}_i\mathbf{W}_i\mathbf{s}_i+\mathbf{z}\Big)\Big),\tag{30}$$

where $\mathbf{z} \sim \mathcal{CN}(0,\sigma_s^2\mathbf{I}_M)$ represents the thermal noise at the MF-RIS. By applying the aggregation beamforming, the computing output at device i is expressed as

$$\hat{\mathbf{s}}_i = \mathbf{A}_i^{\mathrm{H}}\Big(\sum_{c\in\mathcal{C}}\sum_{n\in\mathcal{N}_c}\mathbf{G}_i^{\mathrm{H}}\mathbf{\Theta}_c\mathbf{G}_n\mathbf{W}_n\mathbf{s}_n+\sum_{j\in\mathcal{C}}\mathbf{G}_i^{\mathrm{H}}\mathbf{\Theta}_j\mathbf{z}+\mathbf{z}_i\Big),\tag{31}$$

where $\mathbf{A}_i \in \mathbb{C}^{N_s\times L}$ and $\mathbf{z}_i \sim \mathcal{CN}(0,\sigma_i^2\mathbf{I}_{N_s})$ represent the aggregation matrix and the thermal noise at device i, respectively. Thus, the MSE of device i is defined as

$$\begin{aligned}\mathrm{MSE}_i =& \mathbb{E}(\|\hat{\mathbf{s}}_i-\mathbf{s}\|^2)\\ =&\sum_{c\in\mathcal{C}}\sum_{n\in\mathcal{N}_c}\Big\|\Big(\mathbf{A}_i^{\mathrm{H}}\mathbf{G}_i^{\mathrm{H}}\mathbf{\Theta}_c\mathbf{G}_n\mathbf{W}_n-\frac{1}{N}\mathbf{I}_L\Big)\Big\|^2\\ &+\sum_{j\in\mathcal{C}}\|\mathbf{A}_i^{\mathrm{H}}\mathbf{G}_i^{\mathrm{H}}\mathbf{\Theta}_j\mathbf{z}\|^2+\|\mathbf{A}_i^{\mathrm{H}}\mathbf{z}_i\|^2.\end{aligned}\tag{32}$$

To minimize the average MSE among all users, the optimization problem is formulated by

$$\min_{\mathbf{A},\mathbf{W},\mathbf{\Theta}_c}\frac{1}{N}\sum\nolimits_{i\in\mathcal{N}}\mathrm{MSE}_i(\mathbf{A}_i,\mathbf{W}_i,\mathbf{\Theta}_c)\tag{33a}$$

$$\text{s.t.}\quad \|\mathbf{W}_i\|_F^2 \leq P_i,\tag{33b}$$

$$\|\mathbf{x}_{\mathrm{RIS}}\|^2 \leq P_{\mathrm{RIS}},\tag{33c}$$

$$\beta_m^{r/t}\in[0,\beta_{\max}],\beta_m^r+\beta_m^t\leq\beta_{\max},\theta_m^{r/t}\in[0,2\pi].\tag{33d}$$

The MIMO system involves a higher matrix solving dimension compared to SISO system since each device is equipped with multiple antennas. Moreover, with the non-convex objection function and coupled optimization variables, problem (33) is

challenging to solve directly. Thus, we solve it by decoupling into three subproblems in the following and optimize them iteratively.

B. Algorithm Design

Similar to the SISO case, to address problem (33), we employ the AO technique to optimize one variable at a time while the others fixed in the following.

1) Optimization of Transmit Beamforming: We first optimize the transmit beamforming $\mathbf{W}$ with fixed $\{\mathbf{A}, \mathbf{\Theta}\}$. By ignoring terms without $\mathbf{W}$, we have

$$\begin{aligned}\widetilde{\mathrm{MSE}}_i =& \mathbb{E}(\|\hat{\mathbf{s}}_i - \mathbf{s}\|^2) \\ =& \sum_{c\in\mathcal{C}}\sum_{n\in\mathcal{N}_c} \left\|\left(\mathbf{A}_i^{\mathrm{H}}\mathbf{G}_i^{\mathrm{H}}\mathbf{\Theta}_c\mathbf{G}_n\mathbf{W}_n - \frac{1}{N}\mathbf{I}_L\right)\right\|^2. \end{aligned} \tag{34}$$

Then, we have the following optimization problem

$$\min_{\mathbf{W}} \quad \frac{1}{N}\sum\nolimits_{i\in\mathcal{N}} \widetilde{\mathrm{MSE}}_i(\mathbf{W}) \tag{35a}$$
$$\text{s.t.} \quad (33b),\ (33c). \tag{35b}$$

Defining $\mathbf{W}_c = [\mathbf{W}_1, \mathbf{W}_2, \ldots, \mathbf{W}_{N_c}]^{\mathrm{H}}$, $\bar{\mathbf{G}}_{n,i,c}^{\mathrm{H}} = \mathbf{A}_i^{\mathrm{H}}\mathbf{G}_i^{\mathrm{H}}\mathbf{\Theta}_c\mathbf{G}_n$, and $\widetilde{\mathbf{G}}_{c,i} = [\bar{\mathbf{G}}_{1,i,c}, \bar{\mathbf{G}}_{2,i,c}, \ldots, \bar{\mathbf{G}}_{N_c,i,c}]$, we have

$$\widetilde{\mathrm{MSE}}_i = \sum\nolimits_{c\in\mathcal{C}} \left\|\widetilde{\mathbf{G}}_{c,i}\mathbf{W}_c - \frac{1}{N}\mathbf{I}_{N_c\times 1}\right\|^2. \tag{36}$$

Then, the objective function of problem (35) is given by

$$\begin{aligned}\frac{1}{N}\sum_{i\in\mathcal{N}}\widetilde{\mathrm{MSE}}_i =& \frac{1}{N}\Big(\sum_{c\in\mathcal{C}}\sum_{i\in\mathcal{N}}(\mathrm{Tr}(\mathbf{W}_c^{\mathrm{H}}\widetilde{\mathbf{G}}_{c,i}^{\mathrm{H}}\widetilde{\mathbf{G}}_{c,i}\mathbf{W}_c) \\ &- \frac{2}{N}\mathrm{Re}\{\widetilde{\mathbf{G}}_{c,i}\mathbf{W}_c\} + (\frac{1}{N})^2)\Big). \end{aligned} \tag{37}$$

For constraint (33c), we have

$$\sum\nolimits_{c\in\mathcal{C}} \mathrm{Tr}(\mathbf{W}_c^{\mathrm{H}}\widehat{\mathbf{G}}_c^{\mathrm{H}}\widehat{\mathbf{G}}_c\mathbf{W}_c) \le \bar{P}_{\mathrm{RIS}}, \tag{38}$$

where $\widehat{\mathbf{G}}_c = [\mathbf{\Theta}_c\mathbf{G}_1, \mathbf{\Theta}_c\mathbf{G}_2, \ldots, \mathbf{\Theta}_c\mathbf{G}_{N_c}]$ and $\bar{P}_{\mathrm{RIS}} = P_{\mathrm{RIS}} - \sum_{c\in\mathcal{C}}\sigma_s^2\|\mathbf{\Theta}_c\|^2$. Then, we have

$$\min_{\mathbf{W}} \ \mathrm{Tr}(\mathbf{W}^{\mathrm{H}}\mathbf{G}\mathbf{W}) - 2\,\mathrm{Re}\{\mathrm{Tr}(\bar{\mathbf{B}}\mathbf{W})\} \tag{39a}$$
$$\text{s.t.} \ \ \mathrm{Tr}(\mathbf{W}^{\mathrm{H}}\bar{\mathbf{D}}\mathbf{W}) \le \bar{P}_{\mathrm{RIS}},\ (33b), \tag{39b}$$

where

$$\mathbf{G} = \begin{bmatrix} \frac{1}{N}\sum\limits_{i\in\mathcal{N}}\widetilde{\mathbf{G}}_{r,i}^{\mathrm{H}}\widetilde{\mathbf{G}}_{r,i} & \mathbf{0} \\ \mathbf{0} & \frac{1}{N}\sum\limits_{i\in\mathcal{N}}\widetilde{\mathbf{G}}_{t,i}^{\mathrm{H}}\widetilde{\mathbf{G}}_{t,i}\odot\mathbf{I} \end{bmatrix},\ \mathbf{W} = [\mathbf{W}_r^{\mathrm{H}}, \mathbf{W}_t^{\mathrm{H}}]^{\mathrm{H}},$$

$$\bar{\mathbf{B}} = \Big[\frac{1}{N^2}\sum_{i\in\mathcal{N}}\widetilde{\mathbf{G}}_{r,i}, \frac{1}{N^2}\sum_{i\in\mathcal{N}}\widetilde{\mathbf{G}}_{t,i}\Big],\ \bar{\mathbf{D}} = \begin{bmatrix} \widehat{\mathbf{G}}_r^{\mathrm{H}}\widehat{\mathbf{G}}_r & \mathbf{0} \\ \mathbf{0} & \widehat{\mathbf{G}}_t^{\mathrm{H}}\widehat{\mathbf{G}}_t \end{bmatrix}.$$

Thus, by ignoring constraint (33b), we have the closed form solution of problem (39) as

$$\mathbf{W}^\star = (\mathbf{G} + \xi\bar{\mathbf{D}})^{-1}\bar{\mathbf{B}}^{\mathrm{H}}, \tag{40}$$

where $\xi \ge 0$ is the introduced Lagrange dual variable for the first term in constraint (39b). With constraint (33b), the solution of $\mathbf{W}$ is

$$\begin{aligned}&\mathbf{W}^o_{nL+1:(n+1)L} = \\ &\frac{[\mathbf{W}]^\star_{nL+1:(n+1)L}}{\|[\mathbf{W}]^\star_{nL+1:(n+1)L}\|}\min\Big(\sqrt{P_n}, \|[\mathbf{W}]^\star_{nL+1:(n+1)L}\|\Big), \forall n\in\mathcal{N}. \end{aligned} \tag{41}$$

The lower bound of ξ is $\xi_{LB} = 0$, and the upper bound ξ_{UB} is given by

$$\xi \le \xi_{UB} = \sqrt{\frac{\mathrm{Tr}(\bar{\mathbf{B}}\bar{\mathbf{D}}^{-1}\bar{\mathbf{B}}^{\mathrm{H}})}{\bar{P}_{\mathrm{RIS}}}}. \tag{42}$$

Finally, the optimal ξ can be obtained by the bisection search to ensure the first term in constraint (39b).

2) Optimization of MF-RIS Coefficients: With fixed $\{\mathbf{A}, \mathbf{W}\}$, the corresponding optimization subproblem for $\mathbf{\Theta}_c$ is given by

$$\min_{\mathbf{\Theta}_c} \frac{1}{N}\sum\nolimits_{i\in\mathcal{N}} \mathrm{MSE}_i(\mathbf{\Theta}_c) \tag{43a}$$
$$\text{s.t.}\ (33c),\ (33d). \tag{43b}$$

By only retaining the terms including $\mathbf{\Theta}_c$ in the objective function, we have $\mathrm{MSE}_i(\mathbf{\Theta}_c) = \Psi_i + \Phi_i$, where

$$\begin{aligned}\Phi_i =& \mathrm{Tr}\Big(\sum_{c\in\mathcal{C}}\Big(\sum_{n\in\mathcal{N}_c}\mathbf{A}_i^{\mathrm{H}}\mathbf{G}_i^{\mathrm{H}}\mathbf{\Theta}_c\mathbf{G}_n\mathbf{W}_n\mathbf{W}_n^{\mathrm{H}}\mathbf{G}_n^{\mathrm{H}}\mathbf{\Theta}_c^{\mathrm{H}}\mathbf{G}_i\mathbf{A}_i\Big) \\ &+ \sigma_s^2\sum_{c\in\mathcal{C}}\mathbf{A}_i^{\mathrm{H}}\mathbf{G}_i^{\mathrm{H}}\mathbf{\Theta}_c\mathbf{\Theta}_c^{\mathrm{H}}\mathbf{G}_i\mathbf{A}_i\Big), \end{aligned} \tag{44a}$$

$$\Psi_i = -\frac{2}{N}\mathrm{Tr}\Big(\sum_{c\in\mathcal{C}}\sum_{n\in\mathcal{N}_c}\mathbf{A}_i^{\mathrm{H}}\mathbf{G}_i^{\mathrm{H}}\mathbf{\Theta}_c\mathbf{G}_n\mathbf{W}_n\mathbf{I}_L\Big). \tag{44b}$$

Then, we have $\Psi_i = -\frac{2}{N}\sum_{c\in\mathcal{C}}\mathrm{Re}\{\mathrm{Tr}(\mathbf{R}_{c,i}\mathbf{\Theta}_c)\}$ with

$$\mathbf{R}_{c,i} = \sum\nolimits_{n\in\mathcal{N}_c}\mathbf{G}_n\mathbf{W}_n\mathbf{A}_i^{\mathrm{H}}\mathbf{G}_i^{\mathrm{H}}. \tag{45}$$

Let $\tilde{\mathbf{r}}_{c,i}^{\mathrm{H}} = ([\mathbf{R}_{c,i}]_{1,1}, [\mathbf{R}_{c,i}]_{2,2}, \cdots, [\mathbf{R}_{c,i}]_{M,M})$. We get $\Psi_i = -\frac{2}{N}\sum_{c\in\mathcal{C}}\mathrm{Re}\{\mathrm{Tr}(\tilde{\mathbf{r}}_{c,i}^{\mathrm{H}}\mathbf{u}_c)\}$. Then, we obtain

$$\Phi_i = \sum\nolimits_{c\in\mathcal{C}}\Big(\mathrm{Tr}\Big(\mathbf{T}_{c,i}\mathbf{\Theta}_c\mathbf{\Theta}_c^{\mathrm{H}}\Big) + \mathrm{Tr}\Big(\mathbf{T}_{c,i}\mathbf{\Theta}_c\mathbf{S}_c\mathbf{\Theta}_c^{\mathrm{H}}\Big)\Big), \tag{46}$$

where

$$\mathbf{T}_{c,i} = \sigma_s^2\mathbf{G}_i\mathbf{A}_i\mathbf{A}_i^{\mathrm{H}}\mathbf{G}_i^{\mathrm{H}},\ \mathbf{S}_c = \frac{1}{\sigma_s^2}\sum\nolimits_{n\in\mathcal{N}_c}\mathbf{G}_n\mathbf{W}_n\mathbf{W}_n^{\mathrm{H}}\mathbf{G}_n^{\mathrm{H}}.$$

Based on [39], we have $\mathrm{Tr}(\mathbf{ACBC}^{\mathrm{H}}) = \mathbf{c}^{\mathrm{H}}(\mathbf{A}\odot\mathbf{B}^{\mathrm{T}})\mathbf{c}$, where $\mathbf{A}$ and $\mathbf{B}$ are square matrics, $\mathbf{C}$ is a diagonal matrix with $\mathbf{C} = \mathrm{diag}(\mathbf{c})$. Thus, we have $\Phi_i = \sum_{c\in\mathcal{C}}\mathbf{u}_c^{\mathrm{H}}\widetilde{\mathbf{Q}}_{c,i}\mathbf{u}_c$ with $\widetilde{\mathbf{Q}}_{c,i} = \mathbf{T}_{c,i}\odot(\mathbf{S}_c^{\mathrm{T}} + \mathbf{I}_{M\times M})$. Defining $\widetilde{\mathbf{U}}_c = \mathbf{I}\odot\sigma_s^2\mathbf{S}_c^{\mathrm{T}} + \sigma_s^2\mathbf{I}$, constraint (33c) is recast as $\sum_{c\in\mathcal{C}}\mathbf{u}_c^{\mathrm{H}}\widetilde{\mathbf{U}}_c\mathbf{u}_c \le P_{\mathrm{RIS}}$. After the above variable substitution, problem (43) is equivalently rewritten as

$$\min_{\mathbf{u}_c} \ \frac{1}{N}\sum_{c\in\mathcal{C}}\Big(\mathbf{u}_c^{\mathrm{H}}\sum_{i\in\mathcal{N}}\widetilde{\mathbf{Q}}_{c,i}\mathbf{u}_c - \frac{2}{N}\mathrm{Re}\Big\{\sum_{i\in\mathcal{N}}\tilde{\mathbf{r}}_{c,i}^{\mathrm{H}}\mathbf{u}_c\Big\}\Big) \tag{47a}$$
$$\text{s.t.} \ \ \sum\nolimits_{c\in\mathcal{C}}\mathbf{u}_c^{\mathrm{H}}\widetilde{\mathbf{U}}_c\mathbf{u}_c \le P_{\mathrm{RIS}}, (33d). \tag{47b}$$

By omitting constraint (33d), the Lagrange dual function of problem (47) is given by

$$\mathcal{L} = \mathbf{u}^{\mathrm{H}}\widetilde{\mathbf{Q}}\mathbf{u} - \frac{2}{N}\mathrm{Re}\{\tilde{\mathbf{r}}^{\mathrm{H}}\mathbf{u}\} + \zeta(\mathbf{u}^{\mathrm{H}}\widetilde{\mathbf{U}}\mathbf{u} - P_{\mathrm{RIS}}), \quad (48)$$

where $\zeta \geq 0$ is the introduced Lagrange dual variable for the first term in constraint (47b) and

$$\mathbf{u} = [\mathbf{u}_r, \mathbf{u}_t]^{\mathrm{H}}, \tilde{\mathbf{r}} = \left[\sum\nolimits_{i\in\mathcal{N}} \tilde{\mathbf{r}}_{r,i}, \sum\nolimits_{i\in\mathcal{N}} \tilde{\mathbf{r}}_{t,i}\right]^{\mathrm{H}},$$
$$\widetilde{\mathbf{U}} = \begin{bmatrix} \widetilde{\mathbf{U}}_r & \mathbf{0} \\ \mathbf{0} & \widetilde{\mathbf{U}}_t \end{bmatrix}, \ \widetilde{\mathbf{Q}} = \begin{bmatrix} \sum_{i\in\mathcal{N}} \widetilde{\mathbf{Q}}_{r,i} & \mathbf{0} \\ \mathbf{0} & \sum_{i\in\mathcal{N}} \widetilde{\mathbf{Q}}_{t,i} \end{bmatrix}.$$

By calculating the first-order partial derivation of $\mathcal{L}$ regarding to $\mathbf{u}$, we can obtain

$$\frac{\partial \mathcal{L}}{\partial \mathbf{u}} = 2(\widetilde{\mathbf{Q}} + \varrho\widetilde{\mathbf{U}})\mathbf{u} - \frac{2}{N}\tilde{\mathbf{r}}. \quad (49)$$

Then we have the closed form solution to problem (47) is

$$\mathbf{u}^{\star} = \frac{1}{N}(\widetilde{\mathbf{Q}} + \varrho\widetilde{\mathbf{U}})^{-1}\tilde{\mathbf{r}}. \quad (50)$$

To obtain ϱ, when the first term in constraint (47b) is inactive, we set $\varrho = 0$. If the first term in constraint (47b) is active, we have $\mathbf{u}^{\mathrm{H}}\widetilde{\mathbf{U}}\mathbf{u} = P_{\mathrm{RIS}}$. Then the optimal ζ can be found by the bisection search to ensure $\mathbf{u}^{\mathrm{H}}\widetilde{\mathbf{U}}\mathbf{u} = P_{\mathrm{RIS}}$. The lower bound on ϱ is $\varrho_{LB} = 0$. For the upper bound of ϱ, we have

$$\left(\frac{1}{N}(\widetilde{\mathbf{Q}} + \varrho\widetilde{\mathbf{U}})^{-1}\tilde{\mathbf{r}}\right)^{\mathrm{H}}\widetilde{\mathbf{U}}\left(\frac{1}{N}(\widetilde{\mathbf{Q}} + \varrho\widetilde{\mathbf{U}})^{-1}\tilde{\mathbf{r}}\right) = P_{\mathrm{RIS}}. \quad (51)$$

Since $\zeta\widetilde{\mathbf{U}} \preceq \widetilde{\mathbf{Q}} + \zeta\widetilde{\mathbf{U}}$, we get

$$\left(\frac{1}{N}\right)^2(\varrho^{-1}\widetilde{\mathbf{U}}^{-1}\tilde{\mathbf{r}})^{\mathrm{H}}\widetilde{\mathbf{U}}(\varrho^{-1}\widetilde{\mathbf{U}}^{-1}\tilde{\mathbf{r}}) \geq P_{\mathrm{RIS}}. \quad (52)$$

Because $\mathbf{U}$ is a Hermitian matrix, we obtain

$$\varrho \leq \varrho_{UB} = \sqrt{\frac{\tilde{\mathbf{r}}^{\mathrm{H}}\widetilde{\mathbf{U}}^{-1}\tilde{\mathbf{r}}}{N^2 P_{\mathrm{RIS}}}}. \quad (53)$$

Considering constraint (33d), we have the modified solution of $\mathbf{u}$ as follows

$$\mathbf{u}^{o}_{c,m} = \frac{[\mathbf{u}^{\star}]_{c,m}}{|[\mathbf{u}^{\star}]_{c,m}|}\min\left(\sqrt{\frac{\mathbf{u}^{\star,2}_{c,m}}{\mathbf{u}^{\star,2}_{c,m} + \mathbf{u}^{\star,2}_{\bar{c},m}}\beta_{\max}}, |[\mathbf{u}^{\star}]_{c,m}|\right), \quad (54)$$

where $\bar{c} = r$, if $c = t$, and otherwise. The solution of $\mathbf{u}^{o}_{c,m}$ in (54) is the optimal solution to problem (43).

3) Optimization of Receive Beamforming: With fixed $\{\mathbf{W}, \mathbf{\Theta}_c\}$, the corresponding optimization subproblem regarding to $\mathbf{A}$ is given by

$$\min_{\mathbf{A}} \frac{1}{N}\sum\nolimits_{i\in\mathcal{N}} \mathrm{MSE}_i(\mathbf{A}_i) \quad (55a)$$

Let $\frac{\partial \mathrm{MSE}(\mathbf{A}_i)}{\partial \mathbf{A}_i} = 0$, we have the closed form solution of the optimal $\mathbf{A}_i$ as follows

$$\mathbf{A}_i = (\mathbf{D}_i + \sigma_s^2\mathbf{E}_i + \sigma_i^2\mathbf{I}_{N_s})^{-1}\mathbf{F}_i, \quad (56)$$

where

$$\mathbf{D}_i = \sum\nolimits_{c\in\mathcal{C}}(\sum\nolimits_{n\in\mathcal{N}_c} \mathbf{G}_i^{\mathrm{H}}\mathbf{\Theta}_c\mathbf{G}_n\mathbf{W}_n\mathbf{W}_n^{\mathrm{H}}\mathbf{G}_n^{\mathrm{H}}\mathbf{\Theta}_c^{\mathrm{H}}\mathbf{G}_i),$$
$$\mathbf{E}_i = \sum\nolimits_{c\in\mathcal{C}} \mathbf{G}_i^{\mathrm{H}}\mathbf{\Theta}_c\mathbf{\Theta}_c^{\mathrm{H}}\mathbf{G}_i,$$
$$\mathbf{F}_i = \frac{1}{N}\sum\nolimits_{c\in\mathcal{C}}\left(\sum\nolimits_{n\in\mathcal{N}_c} \mathbf{G}_i^{\mathrm{H}}\mathbf{\Theta}_c\mathbf{G}_n\mathbf{W}_n\right).$$

C. Analysis of Complexity and Convergence

For the calculation of $\mathbf{A}, \mathbf{W}$, and $\mathbf{\Theta}$, the complexities are $\mathcal{O}(N_s^3)$, $\mathcal{O}((NN_s)^3)$, and $\mathcal{O}(8M^3)$, respectively. Since the bisection search is employed to calculate $\mathbf{W}$ and $\mathbf{\Theta}$, the computational complexities are

$$\mathcal{O}(NN_s)^3\log_2\left(\frac{\xi_{UB}}{\epsilon}\right) \text{ and } \mathcal{O}(8M^3)\log_2\left(\frac{\varrho_{UB}}{\epsilon}\right), \quad (58)$$

where ϵ is the bisection search accuracy. Therefore, the overall complexity of the proposed algorithm is

$$\mathcal{O}\left(T\left(N_s^3 + (NN_s)^3\log_2\left(\frac{\xi_{UB}}{\epsilon}\right) + 8M^3\log_2\left(\frac{\varrho_{UB}}{\epsilon}\right)\right)\right), \quad (59)$$

where T denotes the iteration number for convergence.

V. Performance Analysis

In this section, to assess the performance limits of the proposed MF-RIS-aided AirComp system, we analyze the asymptotic performance under extreme cases. To make the analysis tractable and yield insightful results, we consider two general cases of SISO with $M \to \infty$, and MIMO with $M \to \infty$ and $N_s \to \infty$.

A. MF-RIS-Aided SISO-AirComp System

Based on [7] and [37], we assume: 1) A SISO system is considered, i.e., $N_s = 1$; 2) Each MF-RIS element contains the same amplification factor, i.e., $\beta_m^r = \beta_r$, $\beta_m^t = \beta_t$, $\forall m \in \mathcal{M}$, and $\beta_r = \beta_t$, which helps to derive a concise expression for subsequent performance analysis; 3) The i-th device-MF-RIS channel $\mathbf{h}_i$ follows a Rayleigh distribution, i.e., $\mathbf{h}_i \sim \mathcal{CN}(\mathbf{0}, \rho_h^2\mathbf{I})$; 4) Each device i contains the same thermal noise, i.e., $\sigma_i^2 = \sigma_d^2$; 5) The number of RIS elements is sufficiently large, i.e., $M \to \infty$. With these simplifications, by substituting (25) into (6), we have

$$\mathrm{MSE}_i \approx \frac{1}{N} - \frac{1}{N^2}D_i^{-1}\left(\sum_{c\in\mathcal{C}}\sum_{n\in\mathcal{N}_c} H_{n,i,c}v_n\right)\left(\sum_{c\in\mathcal{C}}\sum_{n\in\mathcal{N}_c} H_{n,i,c}^* v_n^*\right), \quad (60)$$

where $D_i = \sum_{c\in\mathcal{C}}\sum_{n\in\mathcal{N}_c}(|v_n H_{n,i,c}|^2 + \sigma_s^2 h_{i,c}) + \sigma_i^2$ with $h_{i,c} = \mathbf{h}_i^{\mathrm{H}}\mathbf{\Theta}_c\mathbf{\Theta}_c^{\mathrm{H}}\mathbf{h}_i$.

Then, we derive a closed form asymptotic MSE for the MF-RIS-aided SISO system.

Theorem 2. *When $M \to \infty$, the MSE of MF-RIS-aided SISO AirComp system is given by*

$$\mathrm{MSE}_{\mathrm{MF}} = \begin{cases} \frac{1}{NM}\frac{2\sigma_s^2\rho_h^2 P_{\mathrm{RIS}} + N\sigma_d^2 P_o\rho_h^2 + 2\sigma_d^2\sigma_s^2}{P_o P_{\mathrm{RIS}}\rho_h^4}, & \text{if } N = 1, \\ \frac{N-1}{N^2}, & \text{else if } N > 1. \end{cases} \quad (61)$$

Proof. Refer to Appendix B. □

Remark 1. *Based on (61), it can be observed that the asymptotic MSE for the MF-RIS-SISO is related to both the transmit power P_o and the amplification power P_{RIS} when $N = 1$. When $P_{\mathrm{RIS}} \to \infty$, the upper bound of the MSE is $\frac{1}{M}\frac{2\sigma_s^2}{P_o\rho_h^2}$, which is independent to the noise power at devices.*

This reveals that when the amplification power is sufficiently large, the MSE only depends on the noise power at the MF-RIS and the channel of device-MF-RIS. Moreover, when $P_o \to \infty$, we have the upper bound of MSE as $\frac{1}{M}\frac{\sigma_d^2}{P_{\rm RIS}\rho_h^2}$, which only includes the noise power at devices and the device-MF-RIS channel. Thus, it implies that noise power σ_d^2 at devices and channel fading effects ρ_h^2, which changes from ρ_h^4 to ρ_h^2, can be suppressed by increasing the amplification power $P_{\rm RIS}$. Furthermore, when $M \to \infty$ with $N = 1$, MSE $\to 0$. This is because there is only one device in the system without interference from other devices. The communication between MF-RIS and the device can be well guaranteed under perfect CSI.

For comparison, we derive the asymptotic MSE for the STAR-RIS-aided SISO system in Theorem 3 under the same settings.

Theorem 3. *When $M \to \infty$, the MSE of STAR-RIS-aided SISO AirComp system is given by*

$$\mathrm{MSE}_{\rm STAR} = \begin{cases} \frac{1}{NM^2}\frac{2\sigma_d^2}{\bar{P}_o\rho_h^4}, & \text{if } N = 1, \\ \frac{N-1}{N^2}, & \text{else if } N > 1, \end{cases} \tag{62}$$

where $\bar{P}_o = P_o + P_{\rm RIS}/N$ for fairness.

Proof. Refer to Appendix C. □

Remark 2. *According to (61) and (62), for $N > 1$, we observe that the MF-RIS and STAR-RIS are approximately inversely proportional to N with $M \to \infty$. When $N = 1$, $\mathrm{MSE}_{\rm MF}$ is inversely proportional to M, while $\mathrm{MSE}_{\rm STAR}$ is inversely proportional to M^2, which is similar to [32]. Thus, when M is sufficiently large, we have $\mathrm{MSE}_{\rm STAR} \geq \mathrm{MSE}_{\rm MF}$. However, with an intermediate size of M, the above result may not hold true. We obtain the number of RIS elements when $\mathrm{MSE}_{\rm STAR} \geq \mathrm{MSE}_{\rm MF}$ in the subsequent corollary.*

Corollary 1. *When $\mathrm{MSE}_{\rm STAR} \geq \mathrm{MSE}_{\rm MF}$, the number of RIS elements M must satisfy*

$$M \geq \frac{P_o}{\bar{P}_o}\frac{2P_{\rm RIS}\sigma_d^2}{2\sigma_s^2\rho_h^2 P_{\rm RIS} + N\sigma_d^2 P_o\rho_h^2 + 2\sigma_d^2\sigma_s^2}, \text{ when } N = 1. \tag{63}$$

Remark 3. *According to (63), denote $\sigma_s^2 = \sigma_d^2 = -80$ dBm, $P_{\rm RIS} = P_o = 10$ mW, $N = 1$, and $\rho_h^2 = -70$ dB. Then we have $\bar{P}_o = P_o + P_{\rm RIS}/N = 20$ mW [37]. The required number of RIS elements M for STAR-RIS to outperform MF-RIS is 3.3×10^6, which is impractical in actual deployment. For $M = 100$, we have $\mathrm{MSE}_{\rm STAR} \approx -20.0$ dB and $\mathrm{MSE}_{\rm MF} \approx -35.2$ dB, which is about 33 times difference.*

B. MF-RIS-Aided MIMO-AirComp System

To further investigate the performance limits under MIMO case[4], we assume: 1) A MIMO system is considered with a significantly large number of transmit/receive antennas and RIS elements, i.e., $N \leq M = N_s \to \infty$; 2) The each entry of the i-th device-MF-RIS channel $\mathbf{G}_i$ follows a Rayleigh distribution, i.e., $\mathcal{CN}(0, \rho_h^2)$; and assumptions 2) and 4) in the last subsection. Besides, we focus on the case with a fixed transmit beamforming, which is given by

$$\mathbf{W}_i^{\rm H}\mathbf{W}_i = \frac{P_o}{L}\mathbf{I}_L, \ \forall i \in \mathcal{N}. \tag{64}$$

With these simplifications, we derive a closed form asymptotic MSE as follows.

Theorem 4. *When $M = N_s \to \infty$, the MSE of MF-RIS-aided MIMO AirComp system is given by*

$$\mathrm{MSE}_{\rm MF} = \begin{cases} \frac{1}{NM}\frac{2\sigma_s^2 P_{\rm RIS}\rho_h^2 + N\sigma_d^2 P_o\rho_h^2 + 2\sigma_d^2\sigma_s^2}{P_o P_{\rm RIS}\rho_h^4}, & \text{if } L = 1, \\ \frac{L-1}{N}, & \text{else if } L > 1. \end{cases} \tag{65}$$

Proof. Refer to Appendix D. □

Then, we provide the asymptotic MSE for the STAR-RIS-aided MIMO system in Theorem 5 under the same settings.

Theorem 5. *When $M = N_s \to \infty$, the MSE of STAR-RIS-aided MIMO AirComp system is given by*

$$\mathrm{MSE}_{\rm STAR} = \begin{cases} \frac{1}{NM^2}\frac{2\sigma_d^2}{P_o\rho_h^4}, & \text{if } L = 1, \\ \frac{L-1}{N}, & \text{else if } L > 1. \end{cases} \tag{66}$$

Proof. Refer to Appendix E. □

Remark 4. *From (65) and (66), we find that when $L = 1$, the asymptotic MSE for MIMO case is similar to the SISO one. However, when $L > 1$, the MSE of both STAR-RIS and MF-RIS is approximately proportional to L, which causes a sharp deterioration in MSE performance with the increase of L. This is because that as the number of functions operated in devices increases, the computation error increases with the severe inter-function interference.*

VI. Simulation Results

In this section, simulation results are provided to evaluate the MSE performance of the proposed algorithm for the considered MF-RIS assisted distributed AirComp system.

A. Simulation Setups

The MF-RIS is located at $(0, 0, 30)$ meter (m), where the devices are uniformly distributed in a circle centered on $(0, 0, 0)$ m with radius equal to 50 m. For the device-MF-RIS links in the SISO case, we consider Rician fading with Rician factor κ. The corresponding channel vector at device i is given by

$$\mathbf{h}_i = \sqrt{\rho(d/d_0)^{-\alpha}}\left(\sqrt{\frac{\kappa}{\kappa+1}}\mathbf{h}_i^{\rm LOS} + \sqrt{\frac{1}{\kappa+1}}\mathbf{h}_i^{\rm NLOS}\right),$$

where $\mathbf{h}_i^{\rm LOS}$ and $\mathbf{h}_i^{\rm NLOS}$ denote the line-of-sight (LoS) and the non-LoS (NLOS) components, respectively. Besides, ρ is the path loss at the reference distance $d_0 = 1$ m, and d denotes the distance between the transmitter and the receiver. Here, κ is the path loss exponent. The device-MF-RIS links in the MIMO case are similar to the setup in the SISO one. Unless otherwise specified, we set $M = 200$, $N = 10$, $N_s = 10$, $L = 4$, $\rho =$

[4]Although the SISO asymptotic MSE expression can be derived from the MIMO one, presenting both cases helps to understand the generality and specialization of the theory, and to deepen the understanding of the overall theoretical framework.

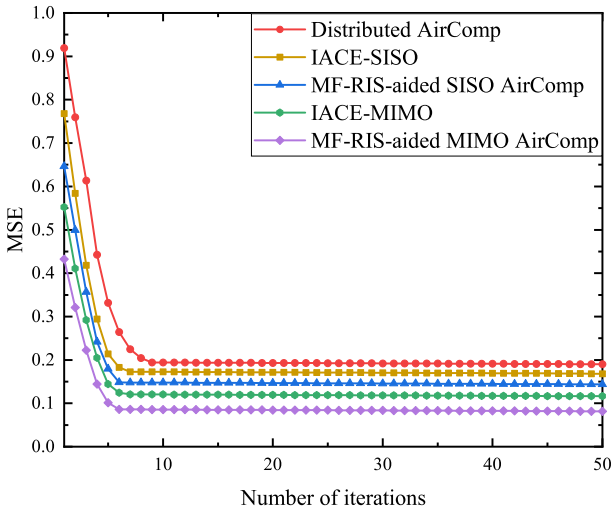

Fig. 3. The convergence performance of the proposed alogorithm.

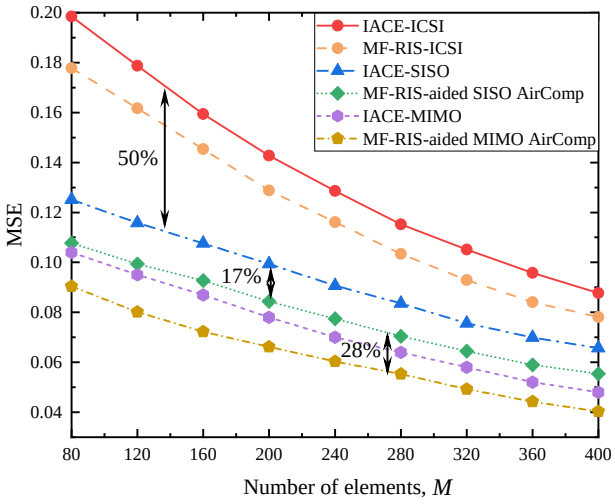

Fig. 4. MSE vs. Number of RIS elements M with $\sigma_{e,i}^2 = 0.1$.

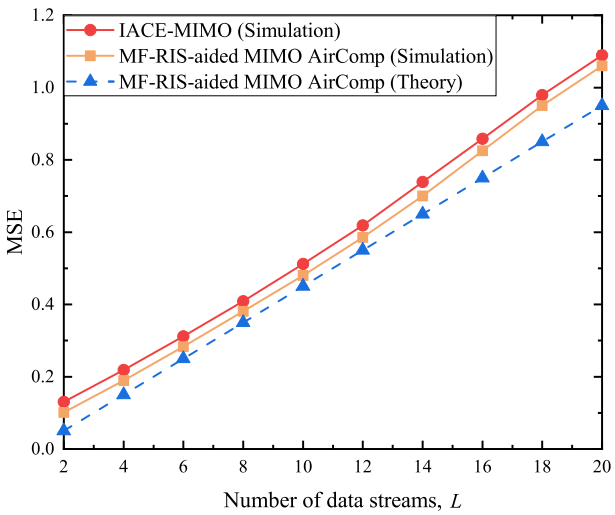

Fig. 5. MSE vs. Number of data streams L.

-30 dB, $\kappa = 10$, $\alpha = 2.2$, $P_o = 10$ dBm, $P_{\text{RIS}} = 10$ dBm, and $\sigma_i^2 = \sigma_s^2 = -80$ dBm [39]. For performance comparison, we consider the following benchmarks:

- Distributed AirComp [6]: For this scheme, we assume that each device communicates with the other remaining devices in the system over a direct link, with no RIS deployment. Similarly, we set the transmit power at each device as $P_o^D = P_o + P_{\text{RIS}}/N$, where N is the number of devices.
- Intelligent AirComp environment (IACE) [33]: To enable all users to be served, this IACE scheme is an expanded variant based on [33], consisting of one reflecting surface and one refracting surface. For fairness, we set the transmit power at each device as $P_o^S = P_o + P_{\text{RIS}}/N$, where N is the number of devices.
- Imperfect CSI (ICSI) [38]: To investigate the MSE performance in the case of imperfect CSI, taking SISO as an example, we set $\widetilde{\mathbf{h}}_i \in \mathbb{C}^{M\times 1}$ as the estimated channel vector for device i [38]. Then we have $\widetilde{\mathbf{h}}_i = \mathbf{h}_i + \mathbf{e}_i, \forall i \in \mathcal{N}$, where $\mathbf{e}_i \in \mathbb{C}^{M\times 1}$ denotes the channel estimation error that is a circularly symmetric complex Gaussian (CSCG) random vector with zeros mean and covariance $\sigma_{e,i}^2\mathbf{I}$.

B. Performance Evaluation

Fig. 3 shows the convergence behavior of the proposed algorithm, where $N_s = 20$, $L = 4$, $M = 200$, and $N = 10$, respectively. It can be observed from Fig. 3 that all schemes converge rapidly in a few iterations, since the semi-closed form or closed form solutions of each subproblem is obtained. Besides, distributed AirComp scheme converges more slowly than other schemes. This is reasonable because each device in distributed AirComp scheme needs to design the beamforming for the other remaining devices to aggregate data, while the other schemes can utilize the RIS for data aggregation, thereby reducing the computational complexity.

Fig. 4 investigates the MSE performance of the considered schemes versus the number of RIS elements M, where $N_s = 10$, $L = 4$, and $N = 20$, respectively. As shown in the figure, the computational MSE of all schemes decreases with the increase of M. This is because more elements leads to higher degrees-of-freedom, thus facilitating the flexibility in designing the beamforming matrix. Moreover, the imperfect CSI schemes are observed to perform the worst, which has a 50% higher MSE than schemes without CSI errors. It is reasonable that the CSI errors will degrade the MSE performance. In addition, although MIMO schemes transmit multiple data streams while SISO schemes only transmit one data stream, we observe that the MSE performance of MIMO schemes outperforms the SISO schemes. Specifically, the MF-RIS-aided MIMO AirComp scheme obtains a 28% MSE reduction than that of SISO one when $M = 280$. This is reasonable since the increase in the number of transmit and receive antennas provides more spatial degrees. Furthermore, the MSE achieved by MF-RIS is lower than those achieved by the IACE scheme, where the MSE obtained by the IACE scheme is 17% higher than MF-RIS when $M = 200$. This is because with the signal amplification function, the former can make use of more spatial diversity.

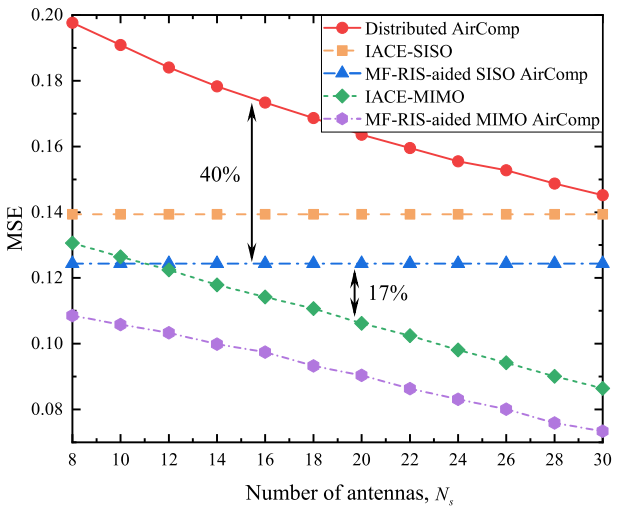

Fig. 6. MSE vs. Number of antennas N_s.

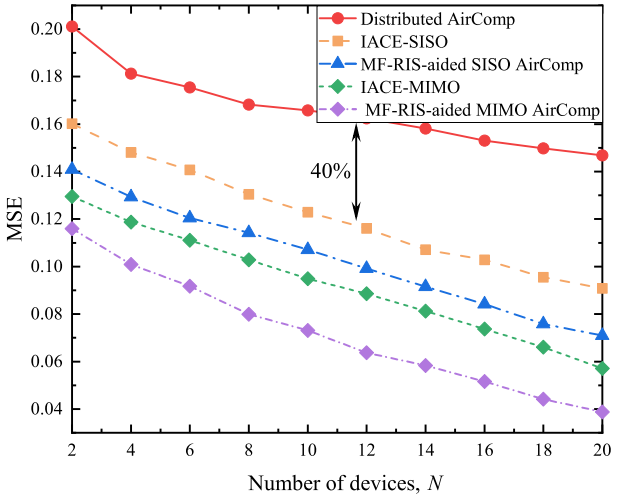

Fig. 7. MSE vs. Number of devices N.

Fig. 5 presents the MSE performance versus the number of data streams L, where $N_s = 20$, $M = 200$, and $N = 20$, respectively. As L increases, the MSE increases rapidly since the number of functions operated at each device increases. This reveals that the multi-function operation will lead to an increased computational error. Besides, we observe that the simulation results coincide well with the derived asymptotic MSE in Section V-B.

Fig. 6 studies the MSE performance versus the number of antennas N_s with $L = 1$, $M = 200$, and $N = 8$. From this figure, we can see that the MSE of the MIMO and distributed AirComp schemes decreases considerably when the number of antennas increases. Particularly, when $N_s \leq 12$, the MF-RIS-aided SISO AirComp scheme is superior to IACE-MIMO scheme. This can be explained as follows. The signal amplification ability of MF-RIS provides more spatial diversity to obtain a better MSE performance than the IACE scheme when N is small. However, as N_s increases, the channel gains between devices tend to be dominant, where the MSE of MF-RIS-aided SISO AirComp increases by 17% compared to the IACE-MIMO when $N_s = 20$. Moreover, distributed AirComp scheme owns the worst MSE performance in all the schemes. In particular, distributed AirComp scheme has a 40% higher MSE than the IACE-SISO scheme when $N_s = 16$. This is because each device in distributed AirComp scheme strives to support N AirComp processes simultaneously despite a limited array size, resulting in an increase in MSE, while the other schemes implement data aggregation with the assistance of RIS.

Fig. 7 plots the MSE performance versus the number of devices N with $L = 2$, $M = 200$, and $N_s = 40$. One can observe that the MSE performance of all considered schemes decreases with N. This coincides with the fact that with the increase of N, the average function can utilize more inter-interference among the devices to improve the MSE performance, as discussed in Section V. Moreover, as N increases, the MSE performance of distributed AirComp scheme gradually saturates, which indicates the cancellation of the opposite effects of aggregation gain in error suppression and severer receive signal misalignment. Specifically, distributed AirComp scheme has a 40% higher MSE than the IACE-SISO scheme when $N = 12$, where the difference becomes larger as N increases. In addition, with the increase of N, the RIS-based schemes, in contrast to distributed AirComp scheme, do not perform a performance floor. This reveals the superiority of RIS-aided distributed AirComp scheme, which is consistent with the discussion in Section V.

VII. Conclusion

In this paper, we investigated an MF-RIS assisted distributed AirComp system. To minimize the computational MSE, we considered SISO and MIMO cases, where the transmit beamforming, receive beamforming, and MF-RIS coefficients are optimized alternately. Then, we obtained the semi-closed form or closed form solutions of each variable by decomposing the original problem into three subproblems. Subsequently, the asymptotic expressions of MSE for SISO and MIMO cases under some reasonable assumptions were derived. Finally, simulation results showed that RIS-aided distributed AirComp systems outperforms distributed AirComp systems without RIS. Moreover, the MF-RIS schemes enjoy a better MSE performance than STAR-RIS schemes, demonstrating the advantages of MF-RIS.

Appendix A
The Derivation for Solving Problem (8)

For constraint (7c), it is a monotonically increasing function with respect to v_n. For objective function of problem (8), the term $\sum_{i\in\mathcal{N}} |(a_i \mathbf{h}_i^{\mathrm{H}} \mathbf{\Theta}_c \mathbf{h}_n v_n - \frac{1}{N})|^2$ is related to a specific $|v_n|$, which is a quadratic function with respect to $|v_n|$. Since v_n^o satisfies constraints (7b) and (7c), the solution v_n^o is the closest feasible point to $v_n^\star$, which is also a feasible point to minimize the objective function (8a). Moreover, under the power constraints (7b) and (7c), the optimal angle of v_n is $-\angle \sum_{i\in\mathcal{N}} a_i \mathbf{h}_i^{\mathrm{H}} \mathbf{\Theta}_c \mathbf{h}_n$ [3].

APPENDIX B
PROOF OF THEOREM 2

We assume the channel vectors of different devices are orthogonal with

$$\lim_{M\to\infty}\frac{1}{M}(\mathbf{h}_n^{\mathrm{H}}\mathbf{h}_n)=\rho_h^2,\ \lim_{M\to\infty}\frac{1}{M}(\mathbf{h}_n^{\mathrm{H}}\mathbf{h}_{\bar{n}})=0.$$

Then we have

$$\begin{aligned}\frac{1}{M^2}(H_{n,i,c}H_{n,i,c}^*)&=\frac{1}{M^2}(\mathbf{h}_i^{\mathrm{H}}\boldsymbol{\Theta}_c\mathbf{h}_n\mathbf{h}_n^{\mathrm{H}}\boldsymbol{\Theta}_c^{\mathrm{H}}\mathbf{h}_i)\\&\approx\frac{\rho_h^2}{M}(\mathbf{h}_i^{\mathrm{H}}\boldsymbol{\Theta}_c\boldsymbol{\Theta}_c^{\mathrm{H}}\mathbf{h}_i)\\&=\frac{\beta_c^2\rho_h^2}{M}(\mathbf{h}_i^{\mathrm{H}}\mathbf{h}_i)\approx\beta_c^2\rho_h^4,\ \forall n\in\mathcal{N},\\\frac{1}{M^2}(H_{n,i,c}^*H_{\bar{n},i,c})&=0,\ \forall n\in\mathcal{N}.\end{aligned}$$

To minimize (60), we set

$$|v_n|^2=P_o,\beta_r^2=\beta_t^2=\frac{P_{\mathrm{RIS}}}{2M(\frac{N}{2}P_o\rho_h^2+\sigma_s^2)}.$$

Then, we get

$$\begin{aligned}\mathrm{MSE}_i=&\frac{1}{N}-\frac{1}{N^2}\Big(\sum_{c\in\mathcal{C}}\sum_{n\in N_c}H_{n,i,c}v_n\Big)D_i^{-1}\Big(\sum_{c\in\mathcal{C}}\sum_{n\in N_c}H_{n,i,c}^*v_n^*\Big)\\=&\frac{1}{N}-\frac{1}{N^2}\frac{\Big(\sum_{c\in\mathcal{C}}\sum_{n\in\mathcal{N}_c}H_{n,i,c}v_n\Big)\Big(\sum_{c\in\mathcal{C}}\sum_{n\in\mathcal{N}_c}H_{n,i,c}^*v_n^*\Big)}{\sum_{c\in\mathcal{C}}\sum_{n\in\mathcal{N}_c}(|v_nH_{n,i,c}|^2+\sigma_s^2h_{i,c})+\sigma_i^2}\\\approx&\frac{1}{N}-\frac{1}{N^2}\frac{M^2P_oN(\beta_r^2+\beta_t^2)\rho_h^4}{M^2P_oN(\beta_r^2+\beta_t^2)\rho_h^4+2M\sigma_s^2\rho_h^2(\beta_r^2+\beta_t^2)+2\sigma_i^2}\\=&\frac{1}{N}-\frac{1}{N^2}\frac{MNP_o\rho_h^4P_{\mathrm{RIS}}}{MNP_o\rho_h^4P_{\mathrm{RIS}}+2\sigma_s^2\rho_h^2P_{\mathrm{RIS}}+N\sigma_i^2P_o\rho_h^2+2\sigma_i^2\sigma_s^2}\\=&\frac{1}{N}\frac{M(N-1)P_oP_{\mathrm{RIS}}\rho_h^4+2\sigma_s^2\rho_h^2P_{\mathrm{RIS}}+N\sigma_i^2P_o\rho_h^2+2\sigma_i^2\sigma_s^2}{MNP_oP_{\mathrm{RIS}}\rho_h^4+2\sigma_s^2\rho_h^2P_{\mathrm{RIS}}+N\sigma_i^2P_o\rho_h^2+2\sigma_i^2\sigma_s^2},\end{aligned}\tag{67}$$

where $\sigma^2=\sum_{c\in\mathcal{C}}\sigma_s^2h_{i,c}+\sigma_i^2$, and we assume $N_r=N_t=\frac{N}{2}$.

Finally, since $\sigma_i^2=\sigma_d^2$, we obtain

$$\mathrm{MSE}=\begin{cases}\frac{1}{NM}\frac{2\sigma_s^2\rho_h^2P_{RIS}+N\sigma_d^2P_o\rho_h^2+2\sigma_d^2\sigma_s^2}{P_oP_{\mathrm{RIS}}\rho_h^4}, & \text{if } N=1,\\\frac{N-1}{N^2}, & \text{else if } N>1.\end{cases}\tag{68}$$

APPENDIX C
PROOF OF THEOREM 3

Let $\sigma_r^2=0$ in D_i, we get

$$\widetilde{D}_i=\sum\nolimits_{c\in\mathcal{C}}\sum\nolimits_{n\in\mathcal{N}_c}|v_nH_{n,i,c}|^2+\sigma_i^2.$$

$$\begin{aligned}\mathrm{MSE}_i\approx&\frac{1}{N}-\frac{1}{N^2}\Big(\sum\nolimits_{c\in\mathcal{C}}\sum\nolimits_{n\in\mathcal{N}_c}H_{n,i,c}v_n\Big)\widetilde{D}_i^{-1}\\&\Big(\sum\nolimits_{c\in\mathcal{C}}\sum\nolimits_{n\in\mathcal{N}_c}H_{n,i,c}^*v_n^*\Big).\end{aligned}$$

Then, by setting set $N_r=N_t=\frac{N}{2}$ and $\bar{P}_o=P_o+P_{RIS}/N$, we have

$$\begin{aligned}\mathrm{MSE}_i=&\frac{1}{N}-\frac{1}{N^2}\widetilde{D}_i^{-1}\Big(\sum_{c\in\mathcal{C}}\sum_{n\in\mathcal{N}_c}H_{n,i,c}v_n\Big)\Big(\sum_{c}\sum_{n\in\mathcal{N}_c}H_{n,i,c}^*v_n^*\Big)\\=&\frac{1}{N}-\frac{1}{N^2}\frac{\Big(\sum_{c\in\mathcal{C}}\sum_{n\in\mathcal{N}_c}H_{n,i,c}v_n\Big)\Big(\sum_{c\in\mathcal{C}}\sum_{n\in\mathcal{N}_c}H_{n,i,c}^*v_n^*\Big)}{\sum_{c\in\mathcal{C}}\sum_{n\in\mathcal{N}_c}|v_nH_{n,i,c}|^2+\sigma_i^2}\\\approx&\frac{1}{N}-\frac{1}{N^2}\frac{M^2\bar{P}_o\frac{N}{2}(\beta_r^2+\beta_t^2)\rho_h^4}{M^2\bar{P}_o\frac{N}{2}(\beta_r^2+\beta_t^2)\rho_h^4+\sigma_i^2}\\=&\frac{1}{N}-\frac{1}{N}\frac{M^2\bar{P}_o\rho_h^4}{M^2N\bar{P}_o\rho_h^4+2\sigma_i^2}\\=&\frac{1}{N}\frac{M^2(N-1)\bar{P}_o\rho_h^4+2\sigma_i^2}{M^2N\bar{P}_o\rho_h^4+2\sigma_i^2},\end{aligned}\tag{69}$$

Then, with $\sigma_i^2=\sigma_d^2$ and $\beta_r^2+\beta_t^2=1$, we get

$$\mathrm{MSE}=\begin{cases}\frac{1}{NM^2}\frac{2\sigma_d^2}{\bar{P}_o\rho_h^4}, & \text{if } N=1,\\\frac{N-1}{N^2}, & \text{else if } N>1.\end{cases}\tag{70}$$

APPENDIX D
PROOF OF THEOREM 4

By substituting (56) into (32), we have

$$\begin{aligned}\mathrm{MSE}_i\approx&\frac{1}{N}-\frac{1}{N^2}\\&\mathrm{Tr}\Big(\sum_{c\in\mathcal{C}}\sum_{n\in\mathcal{N}_c}\mathbf{H}_{n,i,c}^{\mathrm{H}}\mathbf{D}_i^{-1}\sum_{c\in\mathcal{C}}\sum_{n\in\mathcal{N}_c}\mathbf{H}_{n,i,c}\Big),\end{aligned}\tag{71}$$

where $\mathbf{D}_i=\sum_{c\in\mathcal{C}}\sum_{n\in\mathcal{N}_c}(\mathbf{H}_{n,i,c}\mathbf{H}_{n,i,c}^{\mathrm{H}}+\sigma_s^2\mathbf{F}_{i,c}\mathbf{F}_{i,c}^{\mathrm{H}})+\sigma_i^2\mathbf{I}_{N_s}$ with $\mathbf{H}_{n,i,c}=\mathbf{G}_i^{\mathrm{H}}\boldsymbol{\Theta}_c\mathbf{G}_n\mathbf{W}_n$ and $\mathbf{F}_{i,c}=\mathbf{G}_i^{\mathrm{H}}\boldsymbol{\Theta}_c$. Let

$$\lim_{M\to\infty}\frac{1}{M}(\mathbf{G}_n^{\mathrm{H}}\mathbf{G}_n)=\rho_h^2\mathbf{I}_{N_s},\ \lim_{M\to\infty}\frac{1}{M}(\mathbf{G}_n^{\mathrm{H}}\mathbf{G}_{\bar{n}})=\mathbf{0}_{N_s}.$$

Then we assume $\|\mathbf{W}_n\|^2=P_o$ to minimize the target MSE and obtain

$$\begin{aligned}\mathbf{H}_{n,i,c}^{\mathrm{H}}\mathbf{H}_{n,i,c}&=\mathbf{W}_n^{\mathrm{H}}\mathbf{G}_n^{\mathrm{H}}\boldsymbol{\Theta}_c^{\mathrm{H}}\mathbf{G}_i\mathbf{G}_i^{\mathrm{H}}\boldsymbol{\Theta}_c\mathbf{G}_n\mathbf{W}_n\\&\approx M\rho_h^2(\mathbf{W}_n^{\mathrm{H}}\mathbf{G}_n^{\mathrm{H}}\boldsymbol{\Theta}_c^{\mathrm{H}}\boldsymbol{\Theta}_c\mathbf{G}_n\mathbf{W}_n)\\&\approx M\rho_h^2\beta_c^2(\mathbf{W}_n^{\mathrm{H}}\mathbf{G}_n^{\mathrm{H}}\mathbf{G}_n\mathbf{W}_n)\\&=M^2\rho_h^4\beta_c^2(\mathbf{W}_n^{\mathrm{H}}\mathbf{W}_n)\\&\approx M^2\frac{P_o}{L}\beta_c^2\rho_h^4\mathbf{I}_L,\ \forall n\in\mathcal{N},\\\mathbf{H}_{n,i,c}^{\mathrm{H}}\mathbf{H}_{\bar{n},i,c}&\approx\mathbf{0}_L,\ \forall n\in\mathcal{N}.\end{aligned}\tag{72}$$

Thus, let $\boldsymbol{\Theta}_c\boldsymbol{\Theta}_c^{\mathrm{H}}=\beta_c^2\mathbf{I}_M$, we obtain

$$\begin{aligned}\bar{\mathbf{D}}_i&=\Big(\sum_{c\in\mathcal{C}}\sum_{n\in\mathcal{N}_c}(\mathbf{H}_{n,i,c}\mathbf{H}_{n,i,c}^{\mathrm{H}}+\sigma_s^2\mathbf{F}_{i,c}\mathbf{F}_{i,c}^{\mathrm{H}})+\sigma_i^2\Big)\\&\approx\sum_{c\in\mathcal{C}}\Big(\sum_{n\in\mathcal{N}_c}\bar{\mathbf{H}}_{n,i,c}\bar{\mathbf{H}}_{n,i,c}^{\mathrm{H}}+M\sigma_s^2\beta_c^2\rho_h^2\mathbf{I}_{N_s}\Big)+\sigma_i^2\mathbf{I}_{N_s}\\&=\sum_{c\in\mathcal{C}}\sum_{n\in\mathcal{N}_c}\bar{\mathbf{H}}_{n,i,c}\bar{\mathbf{H}}_{n,i,c}^{\mathrm{H}}+\sigma^2\mathbf{I}_{N_s},\end{aligned}$$

where $\bar{\mathbf{H}}_{n,i,c}=\mathbf{H}_{n,i,c},\ \forall n\in\mathcal{N}$, and $\sigma^2=\sum_{c\in\mathcal{C}}M\sigma_s^2\beta_c^2\rho_h^2\mathbf{I}_{N_s}+\sigma_i^2\mathbf{I}_{N_s}$.

Based on the Woodbury matrix identity [**?**], we get

$$\bar{\mathbf{D}}_{i,n}=\begin{cases}\sigma^2, & \text{if } n=0,\\\bar{\mathbf{D}}_{i,n-1}+\bar{\mathbf{H}}_{n,i,c}\bar{\mathbf{H}}_{n,i,c}^{\mathrm{H}}, & \text{else if } n\in N_c.\end{cases}\tag{73}$$

Then we have

$$\bar{\mathbf{D}}_{i,n}^{-1}=\begin{cases}\bar{\mathbf{D}}_{i,n-1}^{-1}-\bar{\mathbf{D}}_{i,n-1}^{-1}\bar{\mathbf{H}}_{n,i,r}(\mathbf{I}+\\\bar{\mathbf{H}}_{n,i,r}^{\mathrm{H}}\bar{\mathbf{D}}_{i,n-1}^{-1}\bar{\mathbf{H}}_{n,i,r})^{-1}\bar{\mathbf{H}}_{n,i,r}^{\mathrm{H}}\bar{\mathbf{D}}_{i,n-1}^{-1}, & \text{if } n\in N_r,\\\bar{\mathbf{D}}_{i,n-1}^{-1}-\bar{\mathbf{D}}_{i,n-1}^{-1}\bar{\mathbf{H}}_{n,i,t}(\mathbf{I}+\\\bar{\mathbf{H}}_{n,i,t}^{\mathrm{H}}\bar{\mathbf{D}}_{i,n-1}^{-1}\bar{\mathbf{H}}_{n,i,t})^{-1}\bar{\mathbf{H}}_{n,i,t}^{\mathrm{H}}\bar{\mathbf{D}}_{i,n-1}^{-1}, & \text{else if } n\in N_t.\end{cases}$$

Let $N_r \geq 2$, we get $\bar{\mathbf{D}}_{i,1}^{-1}, \forall n = 2, \ldots, N_r$,

$$\bar{\mathbf{D}}_{i,1}^{-1} = \frac{1}{\sigma^2}(\mathbf{I} - \bar{\mathbf{H}}_{1,i,r}(\sigma^2 \bar{\mathbf{H}}_{1,i,r} + \bar{\mathbf{H}}_{1,i,r}^{\mathrm{H}} \bar{\mathbf{H}}_{1,i,r})^{-1} \bar{\mathbf{H}}_{1,i,r}^{\mathrm{H}}).$$

Then, since $\bar{\mathbf{H}}_{1,i,r}^{\mathrm{H}} \bar{\mathbf{H}}_{2,i,r} = 0$, $\bar{\mathbf{D}}_{i,2}^{-1}$ is given by

$$\begin{aligned}
\bar{\mathbf{D}}_{i,2}^{-1} &= \bar{\mathbf{D}}_{i,1}^{-1} - \bar{\mathbf{D}}_{i,1}^{-1} \bar{\mathbf{H}}_{2,i,r}(\mathbf{I} + \bar{\mathbf{H}}_{2,i,r}^{\mathrm{H}} \bar{\mathbf{D}}_{i,1}^{-1} \bar{\mathbf{H}}_{2,i,r})^{-1} \bar{\mathbf{H}}_{2,i,r}^{\mathrm{H}} \bar{\mathbf{D}}_{i,1}^{-1} \\
&\approx \bar{\mathbf{D}}_{i,1}^{-1} - \frac{1}{\sigma^2} \bar{\mathbf{H}}_{2,i,r}(\mathbf{I} + \frac{1}{\sigma^2} \bar{\mathbf{H}}_{2,i,r}^{\mathrm{H}} \bar{\mathbf{H}}_{2,i,r})^{-1} \bar{\mathbf{H}}_{2,i,r}^{\mathrm{H}} \\
&= \frac{1}{\sigma^2}(\mathbf{I} - \sum\nolimits_{n=1}^{2} \bar{\mathbf{H}}_{n,i,r}(\sigma^2 \mathbf{I} + \bar{\mathbf{H}}_{n,i,r}^{\mathrm{H}} \bar{\mathbf{H}}_{n,i,r})^{-1} \bar{\mathbf{H}}_{n,i,r}^{\mathrm{H}}).
\end{aligned}$$

Finally, we have

$$\begin{aligned}
\bar{\mathbf{D}}_i^{-1} &= \bar{\mathbf{D}}_{i,N}^{-1} \\
&\approx \frac{1}{\sigma^2}\Big(\mathbf{I} - \sum\nolimits_{c \in \mathcal{C}} \sum\nolimits_{\mathcal{N}_c} \bar{\mathbf{H}}_{n,i,c}(\sigma^2 \mathbf{I} + \bar{\mathbf{H}}_{n,i,c}^{\mathrm{H}} \bar{\mathbf{H}}_{n,i,c})^{-1} \bar{\mathbf{H}}_{n,i,c}^{\mathrm{H}}\Big).
\end{aligned}$$

To minimize (71), we set

$$\beta_r^2 = \beta_t^2 = \frac{P_{\mathrm{RIS}}}{2M(\frac{N}{2}\frac{P_o}{L}\rho_h^2 + \sigma_s^2)}.$$

Thus, we get

$$\begin{aligned}
\mathrm{MSE}_i &= \frac{1}{N} - \frac{1}{N^2} \mathrm{Tr}\Big(\sum_{c \in \mathcal{C}} \sum_{n \in \mathcal{N}_c} \bar{\mathbf{H}}_{n,i,c}^{\mathrm{H}} \bar{\mathbf{D}}_i^{-1} \sum_{c \in \mathcal{C}} \sum_{n \in \mathcal{N}_c} \bar{\mathbf{H}}_{n,i,c}\Big) \\
&\approx \frac{1}{N} - \frac{1}{N^2 \sigma^2} \mathrm{Tr}\Big(\sum_{c \in \mathcal{C}} \sum_{n \in \mathcal{N}_c} \bar{\mathbf{H}}_{n,i,c}^{\mathrm{H}} \\
&\quad \frac{1}{\sigma^2}\Big(\mathbf{I} - \sum_{c \in \mathcal{C}} \sum_{\mathcal{N}_c} \bar{\mathbf{H}}_{n,i,c}(\sigma^2 \mathbf{I} + \bar{\mathbf{H}}_{n,i,c}^{\mathrm{H}} \bar{\mathbf{H}}_{n,i,c})^{-1} \bar{\mathbf{H}}_{n,i,c}^{\mathrm{H}}\Big) \\
&\quad \sum_{c \in \mathcal{C}} \sum_{n \in \mathcal{N}_c} \bar{\mathbf{H}}_{n,i,c}\Big) \\
&\approx \frac{1}{N} - \frac{1}{N^2 \sigma^2} \sum_{c \in \mathcal{C}} \sum_{n \in \mathcal{N}_c} \Big(M^2 \frac{P_o}{L} \beta_c^2 \rho_h^4 \mathbf{I}_L \\
&\quad \Big(\mathbf{I}_{N_s} - \Big(\sigma^2 \mathbf{I}_L + M^2 \frac{P_o}{L} \beta_c^2 \rho_h^4 \mathbf{I}_L\Big)^{-1} M^2 \frac{P_o}{L} \beta_c^2 \rho_h^4 \mathbf{I}_{N_s}\Big)\Big) \\
&= \frac{1}{N} - \frac{1}{N^2 \sigma^2} \sum_{c \in \mathcal{C}} \sum_{n \in \mathcal{N}_c} \Big(M^2 \frac{P_o}{L} \beta_c^2 \rho_h^4 \mathbf{I}_L (\sigma^2 \mathbf{I}_L + M^2 \frac{P_o}{L} \beta_c^2 \rho_h^4 \mathbf{I}_L)^{-1}\Big) \\
&= \frac{1}{N} - \frac{1}{N^2} \mathrm{Tr}\left(\frac{\frac{N}{2} M^2 \frac{P_o}{L} (\beta_r^2 + \beta_t^2) \rho_h^4 \mathbf{I}_L}{\sigma^2 + M^2 \frac{P_o}{L} \beta_c^2 \rho_h^4}\right) \\
&= \frac{1}{N} - \frac{1}{N} \mathrm{Tr}\left(\frac{M \frac{P_o}{L} P_{\mathrm{RIS}} \rho_h^4 \mathbf{I}_L}{2\sigma_s^2 P_{\mathrm{RIS}} \rho_h^2 + N\sigma_i^2 \frac{P_o}{L} \rho_h^2 + 2\sigma_i^2 \sigma_s^2 + M \frac{P_o}{L} P_{\mathrm{RIS}} \rho_h^4}\right) \\
&= \frac{1}{N} \frac{2L\sigma_s^2 P_{\mathrm{RIS}} \rho_h^2 + N\sigma_i^2 P_o \rho_h^2 + 2L\sigma_i^2 \sigma_s^2 + (1-L) M P_o P_{\mathrm{RIS}} \rho_h^4}{2L\sigma_s^2 P_{RIS} \rho_h^2 + N\sigma_i^2 P_o \rho_h^2 + 2L\sigma_i^2 \sigma_s^2 + M P_o P_{\mathrm{RIS}} \rho_h^4} \\
&= \frac{1}{NM} \frac{2L\sigma_s^2 P_{\mathrm{RIS}} \rho_h^2 + N\sigma_i^2 P_o \rho_h^2 + 2L\sigma_i^2 \sigma_s^2 + (1-L) M P_o P_{\mathrm{RIS}} \rho_h^4}{P_o P_{\mathrm{RIS}} \rho_h^4},
\end{aligned}$$

where we set $N_r = N_t = \frac{N}{2}$. Thus, with $\sigma_i^2 = \sigma_d^2$, we have

$$\mathrm{MSE} = \begin{cases} \frac{1}{NM} \frac{2\sigma_s^2 P_{\mathrm{RIS}} \rho_h^2 + N\sigma_d^2 P_o \rho_h^2 + 2\sigma_d^2 \sigma_s^2}{P_o P_{\mathrm{RIS}} \rho_h^4}, & \text{if } L = 1, \\ \frac{L-1}{N}, & \text{else if } L > 1. \end{cases} \tag{74}$$

Appendix E
Proof of Theorem 5

Let $\sigma_r^2 = 0$ in $\mathbf{D}_i$, we obtain

$$\widetilde{\mathbf{D}}_i = \sum_{c \in \mathcal{C}} \sum_{n \in \mathcal{N}_c} |\bar{\mathbf{H}}_{n,i,c}|^2 + \sigma_i^2 \mathbf{I}_{N_s}, \ \beta_r^2 + \beta_t^2 = 1, \sigma^2 = \sigma_i^2 \mathbf{I}_{N_s}.$$

$$\mathrm{MSE}_i \approx \frac{1}{N} - \frac{1}{N^2} \mathrm{Tr}\Big(\sum_{c \in \mathcal{C}} \sum_{n \in \mathcal{N}_c} \bar{\mathbf{H}}_{n,i,c} \widetilde{\mathbf{D}}_i^{-1} \sum_{c \in \mathcal{C}} \sum_{n \in \mathcal{N}_c} \bar{\mathbf{H}}_{n,i,c}^{\mathrm{H}}\Big).$$

Then, we get

$$\begin{aligned}
\mathrm{MSE}_i &= \frac{1}{N} - \frac{1}{N^2} \mathrm{Tr}\Big(\sum_{c \in \mathcal{C}} \sum_{n \in \mathcal{N}_c} \bar{\mathbf{H}}_{n,i,c}^{\mathrm{H}} \bar{\mathbf{D}}_i^{-1} \sum_{c \in \mathcal{C}} \sum_{n \in \mathcal{N}_c} \bar{\mathbf{H}}_{n,i,c}\Big) \\
&\approx \frac{1}{N} - \frac{1}{N^2 \sigma^2} \mathrm{Tr}\Big(\sum_{c \in \mathcal{C}} \sum_{n \in \mathcal{N}_c} \bar{\mathbf{H}}_{n,i,c}^{\mathrm{H}} \frac{1}{\sigma^2}\Big(\mathbf{I} - \sum_{c \in \mathcal{C}} \sum_{\mathcal{N}_c} \bar{\mathbf{H}}_{n,i,c} \\
&\quad \Big(\sigma^2 \mathbf{I} + \bar{\mathbf{H}}_{n,i,c}^{\mathrm{H}} \bar{\mathbf{H}}_{n,i,c}\Big)^{-1} \bar{\mathbf{H}}_{n,i,c}^{\mathrm{H}}\Big) \sum_{c \in \mathcal{C}} \sum_{n \in \mathcal{N}_c} \bar{\mathbf{H}}_{n,i,c}\Big) \\
&\approx \frac{1}{N} - \frac{1}{N^2 \sigma^2} \sum_{c \in \mathcal{C}} \sum_{n \in \mathcal{N}_c} \Big(M^2 \frac{\bar{P}_o}{L} \beta_c^2 \rho_h^4 \mathbf{I}_L \\
&\quad \Big(\mathbf{I}_{N_s} - \Big(\sigma^2 \mathbf{I}_L + M^2 \frac{\bar{P}_o}{L} \beta_c^2 \rho_h^4 \mathbf{I}_L\Big)^{-1} M^2 \frac{\bar{P}_o}{L} \beta_c^2 \rho_h^4 \mathbf{I}_{N_s}\Big)\Big) \\
&= \frac{1}{N} - \frac{1}{N^2 \sigma^2} \sum_{c \in \mathcal{C}} \sum_{n \in N_c} \Big(M^2 \frac{\bar{P}_o}{L} \beta_c^2 \rho_h^4 \mathbf{I}_{N_s} \\
&\quad \Big(\sigma^2 \mathbf{I}_L + M^2 \frac{\bar{P}_o}{L} \beta_c^2 \rho_h^4 \mathbf{I}_L\Big)^{-1}\Big) \\
&= \frac{1}{N} - \frac{1}{N^2} \mathrm{Tr}\left(\frac{\frac{N}{2} M^2 \frac{\bar{P}_o}{L} (\beta_r^2 + \beta_t^2) \rho_h^4 \mathbf{I}_L}{\sigma^2 + M^2 \frac{\bar{P}_o}{L} \beta_c^2 \rho_h^4}\right) \\
&= \frac{1}{N} - \frac{1}{N} \mathrm{Tr}\left(\frac{M^2 \frac{\bar{P}_o}{L} \rho_h^4 \mathbf{I}_L}{2\sigma^2 + M^2 \frac{\bar{P}_o}{L} \rho_h^4}\right) \\
&= \frac{1}{N} \frac{2\sigma_i^2 L + (1-L) M^2 \bar{P}_o \rho_h^4}{2\sigma_i^2 L + M^2 \bar{P}_o \rho_h^4}.
\end{aligned} \tag{75}$$

Thus, with $\sigma_i^2 = \sigma_d^2$, we have

$$\mathrm{MSE} = \begin{cases} \frac{1}{NM^2} \frac{2\sigma_d^2}{\bar{P}_o \rho_h^4}, & \text{if } L = 1, \\ \frac{L-1}{N}, & \text{else if } L > 1. \end{cases} \tag{76}$$

References

[1] J. Lin, *et al.*, "A survey on internet of things: architecture, enabling technologies, security and privacy, and applications," *IEEE Internet Things J.*, vol. 4, no. 5, pp. 1125-1142, Oct. 2017.

[2] G. Zhu, J. Xu, K. Huang, and S. Cui, "Over-the-air computing for wireless data aggregation in massive IoT," *IEEE Wireless Commun.*, vol. 28, no. 4, pp. 57-65, Aug. 2021.

[3] W. Liu, X. Zang, Y. Li, and B. Vucetic, "Over-the-air computation systems: Optimization, analysis and scaling laws," *IEEE Trans. Wireless Commun.*, vol. 19, no. 8, pp. 5488-5502, Aug. 2020.

[4] F. Molinari, N. Agrawal, S. Stanczak, and J. Raisch, "Max-consensus over fading wireless channels," *IEEE Trans. Control. Netw. Syst.*, vol. 8, no. 2, pp. 791-802, Jun. 2021.

[5] W. Ni, Y. Liu, Y. C. Eldar, Z. Yang, and H. Tian, "STAR-RIS integrated non-orthogonal multiple access and over-the-air federated learning: Framework, analysis, and optimization," *IEEE Internet Things J.*, vol. 9, no. 18, pp. 17136-17156, Sept. 2022.

[6] Z. Lin, *et al.*, "Distributed over-the-air computing for fast distributed optimization: Beamforming design and convergence analysis," *IEEE J. Sel. Areas Commun.*, vol. 41, no. 1, pp. 274-287, Jan. 2023.

[7] Q. Wu and R. Zhang, "Intelligent reflecting surface enhanced wireless network via joint active and passive beamforming," *IEEE Trans. Wireless Commun.*, vol. 18, no. 11, pp. 5394-5409, Aug. 2019.

[8] A. Zheng, W. Ni, W. Wang, and H. Tian, "Enhancing NOMA networks via reconfigurable multi-functional surface," *IEEE Commun. Lett.*, vol. 27, no. 4, pp. 1195-1199, Apr. 2023.

[9] X. Cao, G. Zhu, J. Xu, and K. Huang, "Optimized power control for over-the-air computation in fading channels," *IEEE Trans. Wireless Commun.*, vol. 19, no. 11, pp. 7498-7513, Nov. 2020.

[10] X. Zang, W. Liu, Y. Li, and B. Vucetic, "Over-the-air computation systems: Optimal design with sum-power constraint," *IEEE Wireless Commun. Lett.*, vol. 9, no. 9, pp. 1524-1528, Sept. 2020.

[11] L. Chen, X. Qin, and G. Wei, "A uniform-forcing transceiver design for over-the-air function computation," *IEEE Wireless Commun. Lett.*, vol. 7, no. 6, pp. 942-945, Dec. 2018.

[12] L. Chen, N. Zhao, Y. Chen, *et al.*, "Over-the-air computation for IoT networks: Computing multiple functions with antenna arrays," *IEEE Internet Things J.*, vol. 5, no. 6, pp. 5296-5306, Dec. 2018.

[13] G. Zhu and K. Huang, "MIMO over-the-air computation for highmobility multimodal sensing," *IEEE Internet Things J.*, vol. 6, no. 4, pp. 6089-6103, Aug. 2019.

[14] S. Jing and C. Xiao, "Transceiver beamforming for over-the-air computation in massive MIMO systems," *IEEE Trans. Wireless Commun.*, vol. 22, no. 10, pp. 6978-6992, Oct. 2023.

[15] Z. Zhuang, D. Wen, and Y. Shi, "Decentralized over-the-air computation for edge AI inference with integrated sensing and communication," in *Proc. IEEE GLOBECOM*, Kuala Lumpur, Malaysia, Dec. 2023, pp. 4644-4649.

[16] O. Abari, H. Rahul, D. Katabi, and M. Pant, "AirShare: Distributed coherent transmission made seamless," in *Proc. IEEE INFOCOM*, Hong Kong, China, Apr. 2015, pp. 1742-1750.

[17] T. Hou, Y. Liu, Z. Song, X. Sun, Y. Chen, and L. Hanzo, "Reconfigurable intelligent surface aided NOMA networks," *IEEE J. Sel. Areas Commun.*, vol. 38, no. 11, pp. 2575-2588, Nov. 2020.

[18] W. Ni, X. Liu, Y. Liu, H. Tian, and Y. Chen, "Resource allocation for multi-cell IRS-aided NOMA networks," *IEEE Trans. Wireless Commun.*, vol. 20, no. 7, pp. 4253-4268, Jul. 2021.

[19] W. Hao, J. Li, G. Sun, M. Zeng, and O. A. Dobre, "Securing reconfigurable intelligent surface-aided cell-free networks," *IEEE Trans. Inf. Forensics Security*, vol. 17, pp. 3720-3733, Oct. 2022.

[20] Q. Tu, Z. Dong, X. Zou, and N. Wei, "Physical layer security enhancement for mmWave system with multiple RISs and imperfect CSI," *IEICE Trans. Commun.*, vol. E107-B, no. 6, pp. 430-445, Jun. 2024.

[21] Z. Xing, R. Wang, and X. Yuan, "Joint active and passive beamforming design for reconfigurable intelligent surface enabled integrated sensing and communication," *IEEE Trans. Commun.*, vol. 71, no. 4, pp. 2457-2474, Apr. 2023.

[22] Y. Yan, Y. Wang, W. Ni, and D. Niyato, "Joint beamforming design for multi-functional RIS-aided uplink communications," *IEEE Commun. Lett.*, vol. 27, no. 10, pp. 2697-2701, Oct. 2023

[23] W. Wang, W. Ni, and H. Tian, "Multi-functional RIS-aided wireless communications," *IEEE Internet Things J.*, vol. 10, no. 23, pp. 21133-21134, Dec. 2023.

[24] A. Zheng, W. Ni, W. Wang, and H. Tian, "Next-generation RIS: From single to multiple functions," *IEEE Wireless Commun. Lett.*, vol. 12, no. 12, pp. 1988-1992, Dec. 2023.

[25] S. Zhang, W. Hao, G. Sun, C. Huang, Z. Zhu, X. Li, and C. Yuen, "Joint beamforming optimization for active STAR-RIS assisted ISAC systems", Aug. 2023, [online] https://arxiv.org/abs/2308.06064

[26] J. Xie, *et al.*, "Active STARS-assisted rate-splitting multiple-access networks," *Electronics*, vol. 12, no. 18, pp. 3815, Sept. 2023.

[27] W. Fang *et al.*, "Over-the-air computation via reconfigurable intelligent surface," *IEEE Trans. Commun.*, vol. 69, no. 12, pp. 8612-8626, Dec. 2021.

[28] X. Zhai, *et al.*, "Beamforming design based on two-stage stochastic optimization for RIS-assisted over-the-air computation systems," *IEEE Internet of Things J.*, vol. 9, no. 7, pp. 5474-5488, Apr. 2022.

[29] W. Zhang, J. Xu, W. Xu, X. You, and W. Fu, "Worst-case design for RIS-aided over-the-air computation with imperfect CSI," *IEEE Commun. Lett.*, vol. 26, no. 9, pp. 2136-2140, Sept. 2022.

[30] L. Hu, Z. Wang, H. Zhu, Y. Shi, and Y. Zhou, "RIS-assisted over-the-air computation in millimeter wave communication networks," in *Proc. IEEE VTC2022-Spring*, Helsinki, Finland, 2022, pp. 1-5

[31] X. Zhai, G. Han, Y. Cai *et al.*, "Simultaneously transmitting and reflecting (STAR) RIS assisted over-the-air computation systems," *IEEE Trans. Commun.*, vol. 71, no. 3, pp. 1309-1322, Mar. 2023.

[32] D. Zhang, *et al.*, "Beamforming design for active RIS-aided over-the-air computation", Nov. 2023, [online] https://arxiv.org/abs/2311.18418

[33] P. S. Bouzinis, N. A. Mitsiou, P. D. Diamantoulakis, D. Tyrovolas, and G. K. Karagiannidis, "Intelligent over-the-air computing environment," *IEEE Wireless Commun. Lett.*, vol. 12, no. 1, pp. 134-137, Jan. 2023.

[34] W. Ni, A. Zheng, W. Wang, D. Niyato, N. Al-Dhahir, and M. Debbah, "From single to multi-functional RIS: Architecture, key technologies, challenges, and applications," *IEEE Netw.*, vol. 39, no. 1, pp. 38-46, Jan. 2025.

[35] W. Wang, W. Ni, and H. Tian, "Multi-functional RIS-aided wireless communications," *IEEE Internet Things J.*, vol. 10, no. 23, pp. 21133-21134, Dec. 2023.

[36] Z. Zhang, *et al.*, "Full duplex techniques for 5G networks: Self-interference cancellation, protocol design, and relay selection," *IEEE Commun. Mag.*, vol. 53, no. 5, pp. 128-137, May 2015.

[37] Z. Zhang et al., "Active RIS vs. passive RIS: Which will prevail in 6G?," *IEEE Transa. Commun.*, vol. 71, no. 3, pp. 1707-1725, Mar. 2023.

[38] Chen Chen, Emil Björnson, and Carlo Fischione, "Over-the-air computation in cell-free massive MIMO systems," 2024, [online] https://arxiv.org/abs/2409.00517

[39] B. Wei, P. Zhang, and Q. Zhang, "Active reconfigurable intelligent surface-aided over-the-air computation networks," *IEEE Wireless Commun. Lett.*, vol. 13, no. 4, pp. 1148-1152, Apr. 2024.

Ailing Zheng received the B.Eng. degree from Beijing JiaoTong University (BJTU), China, in 2022. She is currently pursuing the M.S. degree in the School of Information and Communication Engineering, Beijing University of Posts and Telecommunications (BUPT). Her research interests include reconfigurable intelligent surface and wireless resource management. She received the National Scholarship twice during her studies at BUPT.

Wanli Ni (Member, IEEE) received the B.Eng. and Ph.D. degrees from Beijing University of Posts and Telecommunications (BUPT), China, in 2018 and 2023, respectively. From 2022 to 2023, he was a visiting Ph.D. student at the Nanyang Technological University, Singapore. He is currently a Postdoctoral Researcher with the Department of Electronic Engineering, Tsinghua University, China. His research interests include federated learning, reconfigurable intelligent surface, semantic communication, edge intelligence, and distributed AI.

He was a recipient of the Outstanding Doctoral Dissertation Awards from both BUPT and China Education Society of Electronics (CESE) in 2023. He was a recipient of the Excellent Graduate of Beijing in 2023. In addition, he received the National Scholarship in 2022 and 2021, and the Samsung Scholarship in 2019. He was a recipient of the Best Paper Award from the IEEE SAGC Conference in 2020. He was a recipient of the IEEE ComSoc Student Travel Grant from multiple international conferences including IEEE INFOCOM, ICC, and GLOBECOM (two times). He was recognized as an IEEE Exemplary Reviewer four times, including IEEE Transactions on Communications in 2022, IEEE Communications Letters in 2022, and IEEE Wireless Communications Letters in 2021 and 2023.

Wen Wang (wangwen@pmlabs.com.cn) received the B.Eng. and Ph.D. degrees from the School of Information and Communication Engineering, Beijing University of Posts and Telecommunications (BUPT), China, in 2020 and 2024, respectively. She received the National Scholarship in 2023, the Huawei Scholarship in 2022, and the Samsung Scholarship in 2021. She is currently a Post-Doctoral Research Fellow with the Pervasive Communications Center, Purple Mountain Laboratories, Nanjing, China, and also with the National Mobile Communications Research Laboratory, Southeast University, Nanjing, China. Her current research interests include wireless resource management and machine learning.

Hui Tian (Senior Member, IEEE) received the M.S. and Ph.D. degrees from Beijing University of Posts and Telecommunications (BUPT), China, in 1992 and 2003, respectively. Currently, she is a professor with the School of Information and Communication Engineering at BUPT. Her current research interests mainly include radio resource management in 5G/6G networks, mobile edge computing, cooperative communication, mobile social network, and Internet of Things.

Yonina C. Eldar Yonina C. Eldar (Fellow, IEEE) received the B.Sc. degree in physics and the B.Sc. degree in electrical engineering from Tel-Aviv University, and the Ph.D. degree in electrical engineering and computer science from MIT, in 2002. She is a Professor with the Department of Mathematics and Computer Science, Weizmann Institute of Science, Rehovot, Israel, where she heads the center for biomedical engineering and signal processing and holds the Dorothy and Patrick Gorman Professorial Chair. She is also a Visiting Professor with MIT, a Visiting Scientist with the Broad Institute, and an Adjunct Professor with Duke University and was a Visiting Professor with Stanford. She is a member of Israel Academy of Sciences and Humanities and a EURASIP Fellow. She has received many awards for excellence in research and teaching, including the IEEE Signal Processing Society Technical Achievement Award (2013), the IEEE/AESS Fred Nathanson Memorial Radar Award (2014) and the IEEE Kiyo Tomiyasu Award (2016). She was a Horev Fellow of the Leaders in Science and Technology Program, the Technion and an Alon Fellow. She received the Michael Bruno Memorial Award from the Rothschild Foundation, the Weizmann Prize for Exact Sciences, the Wolf Foundation Krill Prize for Excellence in Scientific Research, the Henry Taub Prize for Excellence in Research (twice), the Hershel Rich Innovation Award (three times), and the Award for Women with Distinguished Contributions. She received several best paper awards and best demo awards together with her research students and colleagues, was selected as one of the 50 most influential women in Israel, and was a member of the Israel Committee for Higher Education. She is an Editor-in-Chief of Foundations and Trends in Signal Processing, a member of several IEEE Technical Committees and Award Committees, and heads the Committee for Promoting Gender Fairness in Higher Education Institutions in Israel.

Chau Yuen Chau Yuen (S02-M06-SM12-F21) received the B.Eng. and Ph.D. degrees from Nanyang Technological University, Singapore, in 2000 and 2004, respectively. He was a Post-Doctoral Fellow with Lucent Technologies Bell Labs, Murray Hill, in 2005. From 2006 to 2010, he was with the Institute for Infocomm Research, Singapore. From 2010 to 2023, he was with the Engineering Product Development Pillar, Singapore University of Technology and Design. Since 2023, he has been with the School of Electrical and Electronic Engineering, Nanyang Technological University, currently he is Provost's Chair in Wireless Communications, Assistant Dean in Graduate College, and Cluster Director for Sustainable Built Environment at ER@IN.

Dr. Yuen received IEEE Communications Society Leonard G. Abraham Prize (2024), IEEE Communications Society Best Tutorial Paper Award (2024), IEEE Communications Society Fred W. Ellersick Prize (2023), IEEE Marconi Prize Paper Award in Wireless Communications (2021), IEEE APB Outstanding Paper Award (2023), and EURASIP Best Paper Award for JOURNAL ON WIRELESS COMMUNICATIONS AND NETWORKING (2021).

Dr Yuen current serves as an Editor-in-Chief for Springer Nature Computer Science, Editor for IEEE TRANSACTIONS ON VEHICULAR TECHNOLOGY, IEEE TRANSACTIONS ON NEURAL NETWORKS AND LEARNING SYSTEMS, and IEEE TRANSACTIONS ON NETWORK SCIENCE AND ENGINEERING, where he was awarded as IEEE TNSE Excellent Editor Award 2024 and 2022, and Top Associate Editor for TVT from 2009 to 2015. He also served as the guest editor for several special issues, including IEEE JOURNAL ON SELECTED AREAS IN COMMUNICATIONS, IEEE WIRELESS COMMUNICATIONS MAGAZINE, IEEE COMMUNICATIONS MAGAZINE, IEEE VEHICULAR TECHNOLOGY MAGAZINE, IEEE TRANSACTIONS ON COGNITIVE COMMUNICATIONS AND NETWORKING, and ELSEVIER APPLIED ENERGY.

He is listed as Top 2% Scientists by Stanford University, and also a Highly Cited Researcher by Clarivate Web of Science from 2022. He has 4 US patents and published over 500 research papers at international journals.